



Contents lists available at ScienceDirect

Science of the Total Environment

journal homepage: www.elsevier.com/locate/scitotenv

Effects of ocean acidification on acid-base physiology, skeleton properties, and metal contamination in two echinoderms from vent sites in Deception Island, Antarctica

S. Di Giglio^{a,*}, A. Agüera^{a,b}, Ph. Pernet^a, S. M'Zoudi^a, C. Angulo-Preckler^c, C. Avila^d, Ph. Dubois^a

^a Laboratoire de Biologie Marine, Université Libre de Bruxelles, CP 160/15, Avenue F.D. Roosevelt 50, 1050 Bruxelles, Belgium

^b Institute of Marine Research in Norway, Austevoll Research Station, Sauganeset 16, 5392, Norway

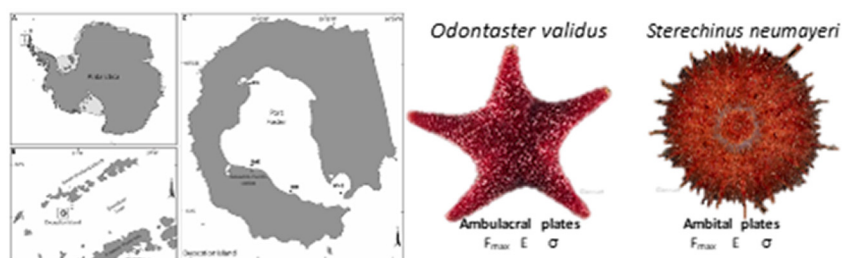
^c Norwegian College of Fishery Science, Faculty of Biosciences, Fisheries and Economics, UiT The Arctic University of Norway, Tromsø, Norway

^d Department of Evolutionary Biology, Ecology and Environmental Sciences, Faculty of Biology and Biodiversity Research Institute (IRBio), Universitat de Barcelona, Av. Diagonal 643, 08028 Barcelona, Catalonia, Spain

HIGHLIGHTS

- Acid-base characteristics of adult Antarctic echinoderms are similar to those of tropical and temperate echinoderms.
- Skeleton properties of both species were weaker than those of tropical and temperate echinoderms.
- Reduced seawater pH and metals had no impact on the skeleton mechanical properties of the two investigated species.
- Reduced pH was correlated to increased contamination by most metals but this relation was weak.

GRAPHICAL ABSTRACT



No impact of low pH and metals on skeleton of both species at Deception Island, West Antarctic Peninsula

ARTICLE INFO

Article history:

Received 26 June 2020

Received in revised form 23 September 2020

Accepted 25 September 2020

Available online xxx

Editor: Julian Blasco

Keywords:

West Antarctic peninsula (WAP)

Echinoderms

Calcification

Marine benthic invertebrates

Mechanical properties

Metals contamination

Ocean acidification

ABSTRACT

Antarctic surface waters are expected to be the first to experience severe ocean acidification (OA) with carbonate undersaturation and large decreases in pH forecasted before the end of this century. Due to the long stability in environmental conditions and the relatively low daily and seasonal variations to which they are exposed, Antarctic marine organisms, especially those with a supposedly poor machinery to eliminate CO₂ and protons and with a heavily calcified skeleton like echinoderms, are hypothesized as highly vulnerable to these environmental shifts. The opportunities offered by the natural pH gradient generated by vent activities in Deception Island caldera, Western Antarctic Peninsula, were used to investigate for the first time the acid-base physiologies, the impact of OA on the skeleton and the impact of pH on metal accumulation in the Antarctic sea star *Odontaster validus* and sea urchin *Sterechinus neumayeri*. The two species were sampled in four stations within the caldera, two at pH (total scale) 8.0–8.1 and two at reduced pH 7.8. Measured variables were pH, alkalinity, and dissolved inorganic carbon of the coelomic fluid; characteristic fracture force, stress and Young's modulus using Weibull statistics and Cd, Cu, Fe, Pb and Zn concentrations in the integument, gonads and digestive system. Recorded acid-base characteristics of both studied species fit in the general picture deduced from temperate and tropical sea stars and sea urchins but conditions and possibly confounding factors, principally food availability and quality, in the studied stations prevented definitive conclusions. Reduced seawater pH 7.8 and metals had almost no impact on the skeleton mechanical properties of the two investigated species despite very high Cd concentrations in *O. validus*

* Corresponding author at: Laboratoire de Biologie Marine, Université Libre de Bruxelles, CP 160/15, Avenue F.D. Roosevelt 50, 1050 Bruxelles, Belgium.
E-mail address: digiglio.sarah@gmail.com (S. Di Giglio).

integument. Reduced pH was correlated to increased contamination by most metals but this relation was weak. Translocation and caging experiments taking into account food parameters are proposed to better understand future processes linked to ocean acidification and metal contamination in Antarctic echinoderms.

© 2020 Elsevier B.V. All rights reserved.

1. Introduction

Human activities are the principal causes of the increasing emissions of global atmospheric carbon dioxide (CO₂) (Andersson et al., 2005; Burns, 2008; Tyrrell, 2011). Atmospheric CO₂ concentration raised from a preindustrial value of 280 ppm to 413 ppm today (August 2020, Ed Dlugokencky and Pieter Tans, NOAA/ESRL (<https://www.esrl.noaa.gov/gmd/ccgg/trends/>)). This CO₂ contributes to global warming although 25–30% are taken up by the oceans (Sabine et al., 2004; Solomon et al., 2008). The ocean absorption of atmospheric CO₂ leads to shifts in the dissolved inorganic carbon (DIC) equilibrium: when the seawater pCO₂ increases (hypercapnia), the pH and carbonate ion concentration decrease (acidosis). By the end of the 21st century, with an expected atmospheric pCO₂ of 485 to 900 ppm, the seawater pH could decrease by up to 0.3–0.4 units (IPCC, 2014; Jewett and Romanou, 2017; Marsh, 2008) and the horizons of saturation of calcium carbonates will locally shoal to the surface (Feely et al., 2004). These modifications are known as ocean acidification (OA) (Caldeira and Wickett, 2003). In turn, these changes in the carbonate system lead to shifts in metal speciation and bioavailability in seawater (Millero et al., 2009).

Surface waters of the Antarctic zone of the Southern Ocean (>60° S) are particularly exposed to these changes because the solubility of CO₂ increases with decreasing temperatures and the Antarctic upwelling brings CO₂ rich water to the surface. Therefore, naturally higher CO₂ and lower carbonate ion concentrations have been already recorded in the Antarctic zone (Monteiro et al., 2020; Sabine et al., 2004). Consequently, Antarctic surface waters are expected to be the first to experience carbonate undersaturation and large decreases in pH (McNeil and Matear, 2008; Steinacher and Joos, 2016). Furthermore, some Antarctic regions are among the most affected by global warming, like the West Antarctic Peninsula (WAP) which is the most rapidly warming region in the Southern hemisphere (IPCC, 2014; Turner et al., 2014; Massom and Stammerjohn, 2010; Montes-Hugo et al., 2009).

Due to the long stability in environmental conditions, including temperature and pH, and the relatively low daily and seasonal variations to which they are exposed, Antarctic marine taxa are hypothesized as vulnerable to environmental shifts, particularly in temperature and pH (Orr et al., 2005; Peck, 2005). Echinoderms include numerous species which play significant ecological roles in the carbon cycling and diversity of the Antarctic macrobenthos (Angulo-Preckler et al., 2018, 2017b; Arntz and Gallardo, 1994; Gutt et al., 1998; Morse et al., 2019; Rogers et al., 2019). Antarctic adult echinoderms were hypothesized to be particularly vulnerable to OA due to their low metabolism - associated to a supposed poor machinery to eliminate CO₂ and protons - and heavily calcified high-magnesium calcite skeleton (McClintock et al., 2011; Sewell and Hofmann, 2011). However, the few available studies on Antarctic echinoderms reported contrasted responses and indicated that they might be more tolerant than expected, at least at the adult stage (Ingels et al., 2012; Constable et al., 2014; Peck, 2018). Under OA, Antarctic sea urchins larvae have been shown to be resilient until pH_{sw} 7.6 (Byrne et al., 2013; Ericson et al., 2010; Foo et al., 2016; Kapsenberg and Hofmann, 2014). On the contrary, the sea star *Odontaster validus* showed negative responses to OA at the larval stage with lower survival and delay of developmental steps (Gonzalez-Bernat et al., 2012). Antarctic adult sea urchins were reported to have the same acid-base characteristics as temperate and tropical species (Collard et al., 2015). Although Dell'Acqua et al. (2019) reported a significant effect on the reproductive condition of the sea urchin *Sterechinus neumayeri* after a short term experiment, a similar decrease of 0.5 pH units for 24 or 40 months had no effect on the

energetics and gonad or test growth of the same species (Suckling et al., 2015; Morley et al., 2016). Currently, no data is available on the acid-base response to OA or on the effects of this on the skeleton of Antarctic echinoderms, which is considered at risk by many authors (McClintock et al., 2011; Sewell and Hofmann, 2011; Duquette et al., 2018).

Shallow hydrothermal vents offer an interesting opportunity to assess the life-long impact of OA by providing gradients of pH established for a long time. These have been extensively used during the last decade in temperate and tropical regions (e.g. Hall-Spencer et al., 2008; Fabricius et al., 2011; Kroeker et al., 2012; Linares et al., 2015; Di Giglio et al., 2020b). Because some of these vents also emit metals, they also allow assessing the impact of OA on metal accumulation by organisms (Bray et al., 2014). To our knowledge, no vent site has been investigated as a surrogate to global change effects in the Southern Ocean. Port Foster, the submerged caldera of Deception Island, South Shetland Islands (WAP), which shows several hydrothermal vents, might be such a site. The presence of several vents could also allow the deconvolution of the effects of temperature, pH, and metals, because different gradients are present (Angulo-Preckler et al., 2018; Deheyn et al., 2005; Guerra et al., 2011; Kusakabe et al., 2009; Somoza et al., 2004). Although environmental conditions of Deception Island might seem hostile for marine life to settle (Berrococo et al., 2018; Flexas et al., 2017) and despite the fact that the island has undergone periodic eruption events throughout its history (Rey et al., 1995), the marine community from Port Foster is rich. It is mainly composed by opportunistic species (bivalves, annelids, amphipods) with the macroepibenthic fauna strongly represented by key echinoderm species such as *Ophionotus victoriae*, *Odontaster validus* and *Sterechinus neumayeri* in very high abundances (Lovell and Trego, 2003; Barnes et al., 2008; Angulo-Preckler et al., 2017a, 2017b, 2018).

The present study used the opportunities offered by the vent activities in Deception Island caldera to address the following questions: (1) is the acid-base physiological answer to acidification of Antarctic echinoderms similar to that of temperate and tropical species; (2) is the skeleton of Antarctic echinoderms affected by acidification as predicted; (3) is metal accumulation by Antarctic echinoderms affected by acidification. We investigated these questions in the two dominant epibenthic echinoderms in the caldera, the sea urchin *S. neumayeri* and the sea star *O. validus*.

2. Materials and methods

2.1. Sampling

Organisms, water and sediment were collected by scuba diving within four stations of Port Foster inside the caldera of Deception Island, South Shetland Islands, West Antarctic Peninsula at the end of February 2018 (Fig. 1). The stations were the same as those described in Angulo-Preckler et al. (2018). Samples were collected at 15 m depth, where temperature and salinity of the seawater were the most stable. Six sea stars *O. validus* Koehler 1906 and six sea urchins *S. neumayeri* (Meissner 1900) were collected alongside with three seawater samples (50 mL) and three sediment samples (500 g, top 2-cm layer) per station. Individuals were maintained in 30 L tanks filled with aerated seawater collected at the same station and immediately brought back to the laboratory and analysed.

Directly after sampling, the physico-chemical characteristics (salinity, temperature, pH and alkalinity) of seawater were measured. Besides, 3 mL seawater were stored in a gas-tight glass tube (Exetainer 3 mL) at 4 °C with 0.5 µL of HgCl₂ (7%) for further measurement of

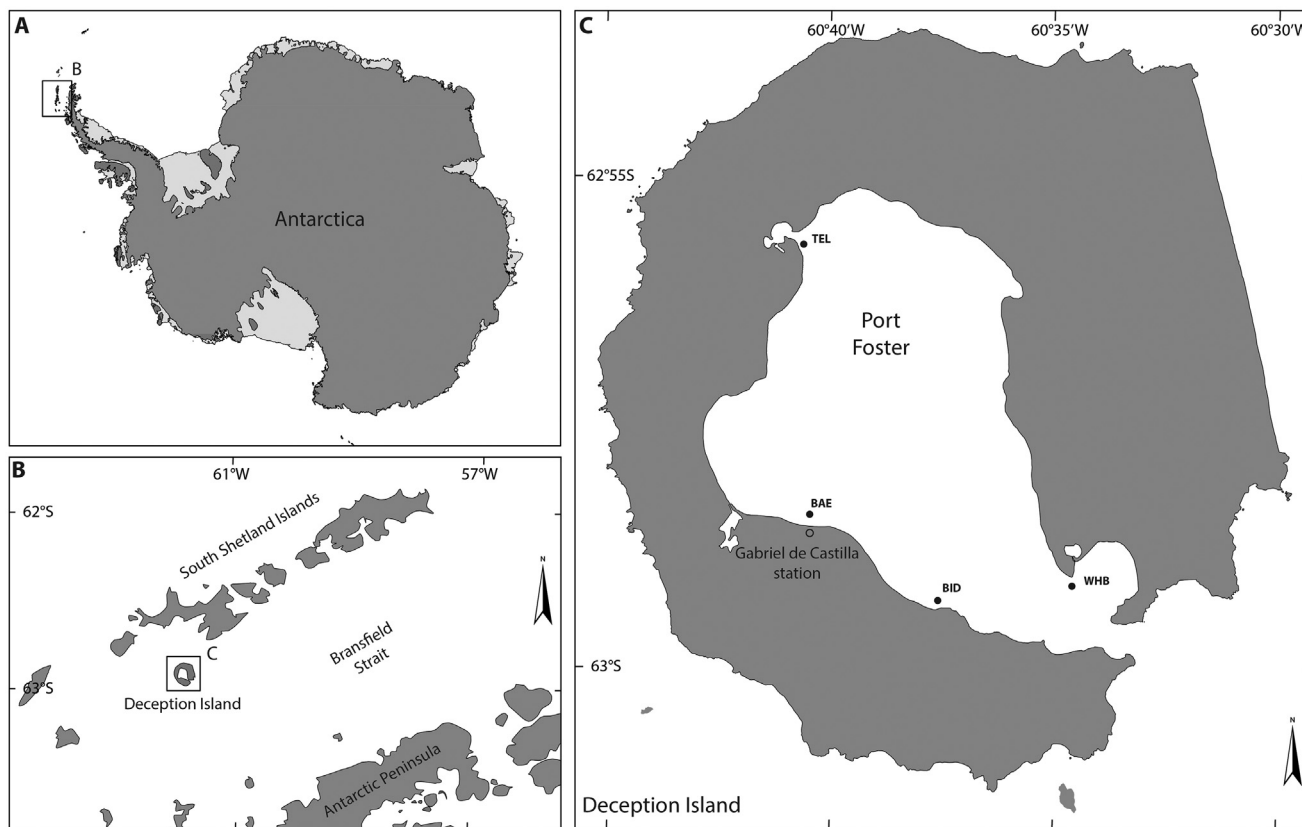


Fig. 1. Sampling area (A) Global map of Antarctica; (B) South Shetland Islands; (C) Deception Island (sampling stations marked with a dot) WHB: Whaler's Bay; BID: Bidones Point; BAE: Antarctic Spanish Base Gabriel de Castilla; Spanish Antarctic Station; TEL: Telephone Bay.

dissolved inorganic carbon concentration (DIC). Sediments were dried in a stove (50 °C for one night) and a part studied as a total fraction. The sediment was stored dried for further metal analysis. All individuals of each species were weighted (wet weight) and measured with a calliper. Also, 3.5 to 6.0 mL of the fluid of the coelomic cavity (= coelomic fluid = CF) was extracted by puncture of the oral membrane with a syringe and a needle. A part of the extracted CF (500 µL) was used to measure the pH while the remaining CF was centrifuged (2000 g for 3 min) at 4 °C and stored with 3 µL HgCl₂ (7%) to avoid other biological activity, for further analysis of DIC. Then, organisms were dissected and the gonads, the integument and the pyloric caeca separated for sea stars; and gonads, integument and digestive tract (emptied of its content) for sea urchins. All the compartments were weighted, dried in an oven at 50 °C for at least 24 h and stored until subsequent analysis of metals or mechanical testing of the skeleton.

2.2. Physico-chemical measurements in seawater and in the coelomic fluid (CF)

All measurements took place in an unheated external lab at Deception Island and samples were maintained on ice when measured. The seawater electromotive force (e.m.f.) was measured using a pH-meter (Metrohm 826 pH mobile) with a combined glass electrode (Metrohm 6.0228.010), while the CF e.m.f. was obtained using a micro-electrode (same pH meter, combined with glass electrode Metrohm 6.0224.100). All measured e.m.f. were then converted to total scale pH according to DelValls and Dickson (1998) method with the calibration based on Tris/AMP buffers. Total alkalinity (TA) of seawater was measured by titration using Gran's function as described in Collard et al. (2013b). To measure the DIC, the samples (CF and seawater) were prepared following the method described in Di Giglio et al. (2020b): 1 µL of phosphoric acid (99%) was deposited on the bottom of a 3 mL empty

Exetainer tube. After the latter tube was flushed with helium for 2 min, 250 µL of the sample were transferred from the sampling tube to the flushed tube using a gas tight syringe. The tubes were stirred for 12 h before analysis. Samples of CO₂ were taken by an automatic sampler (Conflo IV universal continuous flow interface) and analysed in an isotope-ratio mass spectrometer (IRMS, nu instrument) (Gillikin et al., 2010). Parallel to the tubes containing samples of seawater and coelomic fluid, tubes with NaHCO₃ solutions of known concentrations were also measured. These known DIC concentrations were plotted vs. area of the total signal peak of CO₂ detected by the mass spectrometer in order to obtain a calibration curve for DIC in the samples. Analysis of the certified reference material provided by Dickson (batch #151) was within 5.4% of the certified value.

Aragonite and calcite saturation states (Ω) as well as pCO₂ and the concentrations of the carbonate system components in the sea water and these parameters together with TA in the CF were calculated from DIC, pH (total scale), salinity and temperature data (measured in the laboratory and corrected with the field data) using the software CO₂SYS (Pierrot et al., 2006) with the dissociation constants for carbonate from Mehrbach et al. (1973) refitted by (Dickson and Millero (1987), and for KSO₄ from Dickson (1990).

2.3. Metal analyses

Sediment samples (total fraction) and the different compartments from the two species (integument, gonads and pyloric caeca for the sea stars and integument, digestive tract and gonads for the sea urchins) were weighted and a subsample of ca. 0.25 g was oven dried (48 h; 60 °C) at Deception Island. Further experiments took place at the lab of Marine biology at the Université Libre de Bruxelles. Dried sediment samples were placed in acid-washed Teflon vials with Suprapur hydrogen peroxide (H₂O₂) 65% and Suprapure nitric acid 30% (HNO₃) (Sutherland,

2002). Samples were mineralized in a micro-wave oven (MILESTONE 1200 M) using increasing power (250w, 400w, 600w and 800w) – 6 min each. All digested samples were filtered under vacuum on a glass microfiber (Whatman GF/A, retention 1.6 µm, 25 mm diameter) and diluted in MilliQ water to 50 mL. Concentrations of Pb, Cu and Cd were analysed by graphite furnace atomic absorption spectrometry (Varian GTA-100 SpectrAA 6402Z). Concentrations of Zn and Fe were measured by atomic flame absorption spectrometry (GBC 906 AA spectrophotometer). A certified material (278R Community Bureau of Reference Certified Material) mussel soft-tissue powder was analysed with the experimental samples to check the accuracy of the methodology. Analyses of the certified reference material were always within 8.2% of the certified value.

2.4. Ossicle sampling and preparation for mechanical tests

The oven-dried integument of the six sea stars and the six sea urchins per station were cleaned of soft tissues by soaking them into a NaOCl 2.5% solution for 60 min, rinsed with Supra-pure (Sartorius) water and then further soaked in a NaOCl 5.25% solution for 30 min and rinsed with Suprapur water (Sartorius). The solutions were always stirred to prevent the formation of lactic acid and corrosion of the ossicles. The ossicles were air-dried for at least 24 h before their use. The absence of corrosion on plates after the cleaning was checked by observation in a scanning electron microscope (JEOL JSM-7200).

From each individual, five ambulacral plates, i.e. the tube feet holding plates, near the mouth of the sea stars, and five interambulacral ambal plates, i.e. the largest plates of the test, of the sea urchins were sampled. In total, 30 ossicles of each type per species per station were submitted to mechanical tests.

All mechanical tests performed were carried out at room temperature (18 °C). As both types of plates are considered as beams (length is at least ten times the height), we used a three-point bending test, which was carried out as described in Moureaux et al. (2011) and Collard et al. (2016), respectively for sea stars and sea urchins.

Each ossicle was first photographed sideways in front of millimetre paper in order to measure the effective length (length in between the two supporting points) and the thickness of the plates using the ImageJ software (Schneider et al., 2012, Rasband, W.S., U.S. National Institutes of Health, Bethesda, Maryland, USA). They were then placed on a metal stand and the mechanical test was performed using a non-cutting blade fixed on the loading device. It was lowered on the middle of the ambulacral plate and on the primary tubercle of ambal plates at a speed of 0.05 mm min⁻¹ until fracture. One of the two halves of the fractured plates was mounted on an aluminium stub coated with gold and its fracture surface was imaged under scanning electron microscope (JEOL JSM-7200). The second moment of area (I_2) was measured using the macro MomentMacro (developed by Ruff C., Johns Hopkins University School of Medicine, MD, USA) in the software ImageJ (Schneider et al., 2012, Rasband, W.S., U.S. National Institutes of Health, Bethesda, MD, USA). I_2 (m⁴) is a description of the geometric distribution of material around a neutral plane of bending and reflects the proportion of stereom in the plate fracture surface (vs. pores).

$$I_2 = \int y^2 dA \quad (1)$$

where y : the distance to the neutral plane of bending (m) and A : the area (m²).

The apparent Young's modulus, E (Pa), characterizing the material stiffness, was calculated according to the linear-elastic beam theory:

$$E = \frac{F_{max} L_e^3}{48 \Delta L I_2} \quad (2)$$

where: F_{max} : force at fracture (N), ΔL : displacement (m), L_e : effective length (m) and I_2 : second moment of area (m⁴).

The flexural stress of the ossicle in a beam under three-point bending was calculated with:

$$\sigma = E \cdot \varepsilon = \frac{F_{max} L_e^2}{48 I_2} \quad (3)$$

where σ : the bending stress at fracture (Pa), E , Young's modulus (Pa), ε , the strain ($=\Delta L/L$, dimensionless), F_{max} : force at fracture (N), L_e : effective length (m) and I_2 : second moment of area (m⁴).

2.5. Statistical analyses

All ANOVA models and GLM models were built according to the recommendations of Doncaster and Davey (2007) and followed by Tukey test using the appropriate mean square error for multiple comparisons when ANOVA p -value was <0.05.

Physico-chemical parameters of seawater, CF and metals concentration (in the total fraction of the sediments) were analysed with one factor ANOVA (station: fixed factor) for each species separately. Relations between metal concentrations in the different organism compartments and pH in the CF (pH_{CF}) were analysed by canonical correlation analysis. Relationships between contamination (with metals concentration at each station) for all compartments and pH_{CF} were also analysed with principal-component analysis (PCA). Significance of PCA-resulting groups (=stations) was determined using one factor ANOVA on PCA scores of the first and second principal components (PC) separately, and pairwise comparisons were performed using Tukey's test.

Relationships between size (L_e and H) and mechanical properties (F_{max} , I_2 and ΔL) were tested with simple Pearson correlations before performing ANOVAs. L_e was compared according to station using model III ANOVA (station: fixed factor, individual: random factor nested in station). Relations between mechanical properties, pH_{CF} and metal concentrations in the integument were analysed by GLM using as the final model:

$$\text{Considered mechanical variable} = a[\text{Cd}] + b[\text{Pb}] + c[\text{Cu}] + d[\text{Fe}] + e[\text{Zn}] + f \text{pH}_{\text{CF}} + g[\text{Cd}] * \text{pH}_{\text{CF}} + h[\text{Pb}] * \text{pH}_{\text{CF}} + i[\text{Cu}] * \text{pH}_{\text{CF}} + j[\text{Fe}] * \text{pH}_{\text{CF}} + k[\text{Zn}] * \text{pH}_{\text{CF}} + \text{constant} \quad (4).$$

2.6. Weibull analysis

Mechanical properties (F_{max} , Young's modulus (E) and stress (σ)) were analysed using Weibull distribution (the cumulative probability function):

$$P_{f i} = 1 - \exp\left(-\left(\frac{\sigma_i}{\sigma_0}\right)^m\right) \quad (5)$$

where P_f is the probability of failure that increases with the stress variable, σ (Pa). Weibull modulus, m (dimensionless), corresponds to the distribution of flaws within the specimen and the homogeneity of their distribution increased with m . The characteristic stress σ_0 is an experimentally obtained parameter that corresponds to a proportion of fractured samples of $(1-1/e) = 63\%$ (cumulative failure probability). In this study, the characteristic values of the ossicles of each species has been compared according to the stations by using the 95% confidence intervals (CI 95) with the modified least square regression of Bütikofer et al. (2015) and following the methods described by Di Giglio et al. (2020a).

3. Results

Detailed statistical results are presented as supplementary information (Tables S01 to S15).

Table 1

Seawater physico-chemical parameters at the four stations of Deception Island on the day of sampling (Mean \pm SD, $n = 3$). TA, $p\text{CO}_2$, HCO_3^- , CO_3^{2-} , Ω_{calcite} and $\Omega_{\text{aragonite}}$ were calculated with CO2SYS software with pH_T and DIC values. Means sharing the same superscript are not significantly different ($\alpha = 0.05$).

Station	BAE	WHB	BID	TEL	P_{ANOVA}
Temperature ($^{\circ}\text{C}$)	1.5 \pm 0.0	1.0 \pm 0.0	1.1 \pm 0.0	0.7 \pm 0.0	–
Salinity (PSU)	33.0 \pm 0.5a	32.9 \pm 0.1a	32.0 \pm 0.0b	32.3 \pm 0.3b	$<10^{-3}$
pH_T	8.04 \pm 0.01b	8.13 \pm 0.02a	7.77 \pm 0.03c	7.83 \pm 0.04c	$<10^{-3}$
TA (μmolkg^{-1})	2298 \pm 88b	2442 \pm 74b	2399 \pm 103b	2839 \pm 326a	0.028
DIC (mM)	2.28 \pm 0.12b,c	2.76 \pm 0.30a,b	2.13 \pm 0.12c	2.81 \pm 0.15a	0.005
$p\text{CO}_2$ (μatm)	415 \pm 12b	404 \pm 33b	722 \pm 63a	829 \pm 90a	$<10^{-3}$
HCO_3^- (μmolkg^{-1})	2154 \pm 109b,c	2590 \pm 282a,b	2035 \pm 114c	2688 \pm 143a	0.005
CO_3^{2-} (μmolkg^{-1})	98 \pm 9b	141 \pm 20a	48 \pm 4c	72 \pm 7b,c	$<10^{-3}$
$\Omega_{\text{calcite}} = \Omega_{\text{Ca}}$	2.36 \pm 0.20b	3.41 \pm 0.49a	1.16 \pm 0.09c	1.75 \pm 0.18b,c	$<10^{-3}$
$\Omega_{\text{aragonite}} = \Omega_{\text{Ar}}$	1.48 \pm 0.13b	2.14 \pm 0.31a	0.73 \pm 0.06c	1.10 \pm 0.11b,c	$<10^{-3}$

3.1. Seawater physico-chemical parameters and metal concentrations in the sediment

Temperature did not differ between the studied stations. Mean seawater pH_T ranged between 7.77 and 8.13 (Table 1, S01). BAE and WHB, considered as control stations, showed the highest pH_T whereas BID and TEL stations had a significantly lower pH ($P_{\text{ANOVA}} < 10^{-3}$, $P_{\text{Tukey}} \leq 0.023$). Consistently, $p\text{CO}_2$ at BID and TEL was significantly higher than at BAE and WHB stations ($P_{\text{ANOVA}} < 10^{-3}$, $P_{\text{Tukey}} < 10^{-3}$). Mean TA_{SW} ranged between 2298 and 2839 $\mu\text{mol kg}^{-1}$ (Table 1). TA_{SW} was significantly higher at TEL than at the other stations ($P_{\text{ANOVA}} = 0.028$, $P_{\text{Tukey}} \leq 0.041$), where TA_{SW} of other stations did not significantly differ ($P_{\text{Tukey}} \geq 0.073$). DIC from TEL was significantly higher than that of BAE and BID but not of WHB ($P_{\text{ANOVA}} = 0.005$, $P_{\text{Tukey}} \leq 0.034$). The concentration in bicarbonate ions differed between the stations ($P_{\text{ANOVA}} = 0.005$) and followed the same trend as DIC. The concentration in carbonate ions (CO_3^{2-}) significantly differed between the stations ($P_{\text{ANOVA}} < 10^{-3}$), being the highest at WHB ($P_{\text{Tukey}} \leq 0.013$) and the lowest at BID and TEL ($P_{\text{Tukey}} \leq 0.041$). WHB was characterized by the highest Ω_{Ca} and Ω_{Ar} (3.41 and 2.14 respectively, $P_{\text{ANOVA}} < 10^{-3}$, $P_{\text{Tukey}} \leq 0.013$). Values of Ω_{Ca} and Ω_{Ar} at BAE and TEL were not significantly different ($P_{\text{Tukey}} \geq 0.157$). Also, Ω_{Ca} and Ω_{Ar} at TEL and BID were not significantly different ($P_{\text{Tukey}} \geq 0.777$) but BID was characterized by significantly lower Ω_{Ca} and Ω_{Ar} than those at WHB and BAE ($P_{\text{Tukey}} \leq 0.042$).

Metals concentration (Cd, Cu, Fe, Pb and Zn) in the sediment were the highest at WHB (Table 2). The concentrations of Fe and Zn were significantly higher in this station than in all others ($P_{\text{ANOVA}} \leq 0.08$, $P_{\text{Tukey}} \leq 0.022$, Table 2, S02). TEL was systematically the station that presented the smallest concentrations in metals. The Pb concentration in WHB sediment was significantly higher than that in BAE and BID sediments ($P_{\text{Tukey}} \leq 0.036$). Cd concentrations in sediment only differed between WHB and TEL.

The relation between seawater pH and metals concentration in the sediment was tested by principal-component analysis (S03, S04). PC1 explained 73.9% of variance and metal concentrations contributed equally to this PC (~17% each metal with 21.3% for Zn), while PC2 explained 11.1% of variance and pH of seawater contributed the most to this PC (55.6%). Stations differed according to PC1 and PC2

Table 2

Metals concentrations in the sediment (total fraction) at the four stations of Deception Island (West Antarctic Peninsula) on the day of organism sampling (Mean \pm SD, $n = 3$). Means sharing the same superscript are not significantly different ($\alpha < 0.05$).

Total fraction	BAE	WHB	BID	TEL	P_{ANOVA}
[Cd] ($\mu\text{g g}^{-1}$)	0.06 \pm 0.01a,b	0.12 \pm 0.03a	0.06 \pm 0.02a,b	0.04 \pm 0.01b	0.048
[Cu] ($\mu\text{g g}^{-1}$)	6.74 \pm 0.02a,b	9.33 \pm 0.93a	6.67 \pm 0.97a,b	5.16 \pm 0.20b	0.029
[Fe] ($\mu\text{g g}^{-1}$)	9760 \pm 1682b	15,814 \pm 581a	10,271 \pm 1091b	11,277 \pm 1711b	0.008
[Pb] ($\mu\text{g g}^{-1}$)	0.53 \pm 0.10b	1.13 \pm 0.14a	0.67 \pm 0.03b	0.74 \pm 0.20a,b	0.011
[Zn] ($\mu\text{g g}^{-1}$)	29.14 \pm 0.24b	40.57 \pm 1.74a	30.17 \pm 2.56b	28.67 \pm 2.89b	0.001

($P_{\text{ANOVA}} < 10^{-3}$) with WHB being significantly different from the other stations according to PC1 and from BID and TEL according to PC2 ($P_{\text{Tukey}} 0.018$). Seawater pH appeared poorly linked to metal concentrations in the sediment.

3.2. Acid-base physiology of the coelomic fluid (CF) and size of *O. validus* and *S. neumayeri*

Sea stars from WHB had significantly longer arms than those of TEL (Table 3, S05, $P_{\text{ANOVA}} = 0.031$, $P_{\text{Tukey}} \leq 0.038$). Nevertheless, mean $\text{pH}_{T\text{-CF}}$ of *O. validus* was not correlated with the length of the arm of the collected specimens ($P_{\text{Bonferroni}} = 0.288$) and did not significantly differ between organisms from different stations ($P_{\text{ANOVA}} = 0.080$) ranging between 7.65 and 7.77. Similarly, TA, DIC, $p\text{CO}_2$ and bicarbonate ion concentrations of the CF did not differ between sea stars from the four stations ($P_{\text{ANOVA}} \geq 0.064$, S03). However, carbonate ion concentration and consequently Ω_{Ca} and Ω_{Ar} measured in the CF of *O. validus* were significantly different between stations ($P_{\text{ANOVA}} \leq 0.005$). Sea stars from BID showed significantly lower carbonate ion concentrations, Ω_{Ca} , and Ω_{Ar} than those from WHB and TEL but not from those of BAE. Sea stars from BAE, WHB and TEL did not differ for these variables.

Sea urchins height and diameter did not differ significantly between stations ($P_{\text{ANOVA}} \geq 0.151$, Table 3, S06) and were not significantly correlated with the pH of the CF ($P_{\text{Bonferroni}} \geq 0.263$). Mean $\text{pH}_{T\text{-CF}}$ of *S. neumayeri* from BID and TEL were significantly lower than those from sea urchins from WHB but not BAE ($P_{\text{ANOVA}} = 0.003$, $P_{\text{Tukey}} \leq 0.008$). TA of sea urchins from WHB was significantly higher than TA of sea urchins from BAE but not from BID and TEL ($P_{\text{ANOVA}} = 0.003$, $P_{\text{Tukey}} \text{ BAE-WHB} = 0.022$, $P_{\text{Tukey}} \text{ others} \geq 0.315$). DIC measures in the CF of sea urchins from BAE was the lowest and was significantly different from that of sea urchins from WHB and TEL ($P_{\text{ANOVA}} = 0.015$, $P_{\text{Tukey}} \leq 0.026$). ANOVA on $p\text{CO}_2$ measured in the CF of sea urchins was significant, however Tukey tests did not highlight any significant differences ($P_{\text{ANOVA}} = 0.035$, $P_{\text{Tukey}} \geq 0.057$). The concentration in bicarbonate ions of the CF of sea urchins from BAE was significantly lower than that of sea urchins from WHB and TEL ($P_{\text{ANOVA}} = 0.005$, $P_{\text{Tukey}} \leq 0.033$). The concentration in carbonate ions as well as Ω_{Ca} and

Table 3

Acid-base physiology of the coelomic fluid and size of *Odontaster validus* and *Sterechinus neumayeri* from the four stations of Deception Island (Mean \pm SD, $n = 6$ except TA: $n = 3$). $p\text{CO}_2$, $[\text{HCO}_3^-]$, $[\text{CO}_3^{2-}]$, values of Ω_{calcite} and $\Omega_{\text{aragonite}}$ were calculated using CO2SYS software with pH_T and DIC values. Means sharing the same superscript are not significantly different ($\alpha = 0.05$). * Tukey test not significant ($p \geq 0.057$).

Station	BAE	WHB	BID	TEL	P_{ANOVA}
<i>Odontaster validus</i>					
pH_T	7.68 \pm 0.11	7.77 \pm 0.08	7.65 \pm 0.08	7.74 \pm 0.06	0.080
TA (μmolkg^{-1})	2641 \pm 322.46	3054 \pm 217	2566 \pm 263	3253 \pm 834	0.064
DIC (mM)	2.63 \pm 0.32	3.02 \pm 0.23	2.57 \pm 0.28	3.23 \pm 0.85	0.090
pCO_2 (μatm)	1129 \pm 325.05	1056 \pm 217	1205 \pm 372	1208 \pm 450	0.858
HCO_3^- (μmolkg^{-1})	2512 \pm 301.90	2887 \pm 218	2457 \pm 266	3090 \pm 814	0.086
CO_3^{2-} (μmolkg^{-1})	52 \pm 16a,b	69 \pm 13a	43 \pm 6b	67 \pm 12a	0.004
$\Omega_{\text{calcite}} = \Omega_{\text{Ca}}$	1.24 \pm 0.39a,b	1.67 \pm 0.31a	1.05 \pm 0.15b	1.62 \pm 0.30a	0.005
$\Omega_{\text{aragonite}} = \Omega_{\text{Ar}}$	0.78 \pm 0.24a,b	1.04 \pm 0.20a	0.66 \pm 0.09b	1.02 \pm 0.19a	0.004
Arm length (mm)	48.6 \pm 5.1a,b	54.3 \pm 4.7a	49.9 \pm 5.0a	46.0 \pm 2.5b	0.031
<i>Sterechinus neumayeri</i>					
pH_T	7.80 \pm 0.08a,b	7.92 \pm 0.05a	7.69 \pm 0.12b	7.72 \pm 0.13b	0.003
TA (μmolkg^{-1})	4045 \pm 360b	6095 \pm 714a	4617 \pm 946a,b	5539 \pm 1277a,b	0.003
DIC (mM)	3.99 \pm 0.35b	5.85 \pm 0.66a	4.63 \pm 0.98a,b	5.54 \pm 1.28a	0.015
pCO_2 (μatm)	1274 \pm 235*	1418 \pm 163*	2005 \pm 820*	2209 \pm 809*	0.035
HCO_3^- (μmolkg^{-1})	3810 \pm 332b	5668 \pm 650a	4421 \pm 936a,b	5286 \pm 1225a	0.005
CO_3^{2-} (μmolkg^{-1})	102 \pm 22.28b	195 \pm 36a	87 \pm 21b	114 \pm 42b	$<10^{-3}$
$\Omega_{\text{calcite}} = \Omega_{\text{Ca}}$	2.47 \pm 0.54b	4.70 \pm 0.87a	2.10 \pm 0.50b	2.76 \pm 1.02b	$<10^{-3}$
$\Omega_{\text{aragonite}} = \Omega_{\text{Ar}}$	1.55 \pm 0.34b	2.94 \pm 0.54a	1.31 \pm 0.31b	1.73 \pm 0.64b	$<10^{-3}$
D test (mm)	40.7 \pm 1.6	37.8 \pm 6.4	39.3 \pm 3.4	40.3 \pm 1.3	0.286
H test (mm)	23.8 \pm 1.4	20.7 \pm 0.6	23.8 \pm 1.2	23.1 \pm 1.9	0.151

Ω_{Ar} in the CF of sea urchins from WHB were significantly higher than in the other stations ($P_{\text{ANOVA}} < 10^{-3}$, $P_{\text{Tukey}} \leq 0.007$).

3.3. Morphometry and mechanical properties of the skeleton

3.3.1. *Odontaster validus* ambulacral plates

The effective length of the tested plates was not significantly different between sea stars from the different stations (Table 4, S07, $P_{\text{ANOVA}} = 0.204$). However, plates of sea stars from BID were thicker than those from sea stars of TEL ($P_{\text{ANOVA}} = 0.013$, $P_{\text{Tukey}} = 0.022$). The force at fracture (F_{max}) of the ambulacral plates was not correlated with neither arm length of the sea star nor the length or height of the plate ($P_{\text{Bonferroni}} \geq 0.184$). The second moment of area (I_2) was significantly lower in plates of sea stars from BAE than in those from BID ($P_{\text{ANOVA}} = 0.038$, $P_{\text{Tukey}} \leq 0.037$). Characteristic stress (σ_0) obtained by Weibull analyses of ambulacral plates from sea stars of BID were significantly lower than those calculated for sea stars of WHB but not from those obtained for sea stars of BAE, both control stations (Table 5, Fig. 2, S08). The characteristic force at fracture (F_{max0}) was significantly the highest in sea stars from WHB and the lowest in those from BID, with values in TEL and BAE sea stars being intermediate. The characteristic Young's modulus (E_0) of ambulacral plates was significantly lower in sea stars from BID compared to BAE and intermediate in WHB and TEL sea stars. The Weibull moduli did not differ according to station (Table 5, Fig. 3, S08).

Table 4

Effects of ocean. Morphometrical (effective length: L_e , height: H, second moment of inertia: I_2) properties of the ambulacral plates of *Odontaster validus* and the ambital plates of *Sterechinus neumayeri*, at the four stations of Deception Island (Mean \pm SD, $n = 6$). Means sharing the same superscript are not significantly different ($\alpha = 0.05$). * Tukey test not significant ($p \geq 0.084$).

Station	BAE	WHB	BID	TEL	P_{ANOVA}
<i>Odontaster validus</i>					
L_e (10^{-3} m)	3.09 \pm 0.31	3.12 \pm 0.24	3.03 \pm 0.16	2.80 \pm 0.37	0.204
H (10^{-3} m)	0.54 \pm 0.07a,b	0.58 \pm 0.06a,b	0.63 \pm 0.07a	0.49 \pm 0.08b	0.013
I_2 (10^{-15} m ⁴)	5.00 \pm 1.85b	7.44 \pm 1.48a,b	7.92 \pm 1.71a	7.14 \pm 1.96a,b	0.038
<i>Sterechinus neumayeri</i>					
L_e (10^{-3} m)	6.82 \pm 0.16	6.16 \pm 0.55	6.48 \pm 0.11	6.67 \pm 0.69	0.746
H (10^{-3} m)	0.38 \pm 0.03	0.33 \pm 0.03	0.38 \pm 0.04	0.34 \pm 0.04	0.193
I_2 (10^{-15} m ⁴)	2.39 \pm 1.02	2.30 \pm 1.12	2.16 \pm 0.71	2.15 \pm 0.65	0.710

3.3.2. *Sterechinus neumayeri* ambital plates

No morphometrical properties of the ambital plates differed according to stations ($P_{\text{ANOVA}} \geq 0.070$, Table 5, S09). There was no significant correlation between the height or the diameter of the test and the F_{max} of the ambital plates ($P_{\text{Bonferroni}} \geq 0.380$). The length and the height of the ambital plates were not significantly correlated with their F_{max} ($P_{\text{Bonferroni}} \geq 0.503$). The characteristic force at fracture (F_{max0}) of ambital plates of sea urchins was significantly lower in ambital plates of sea urchins from TEL compared to those of the two control stations (Table 5, Fig. 2, S10). The same variable did not differ in sea urchins from BID compared to those from the control stations. Other mechanical properties of ambital plates compared with Weibull statistics, i.e. the

Table 5

Characteristic stress (σ_0), Weibull modulus (m: slope of the linearized Weibull curve), characteristic force at fracture (F_{max0}) and characteristic Young's modulus (E_0) of the ambulacral plates of *Odontaster validus* and the ambital plates of *Sterechinus neumayeri* at the four stations of Deception Island, and their respective 95% confidence intervals (CI 95% \pm : lower and upper limits of 95% confidence interval). Characteristic values sharing the same superscript are not significantly different based on their respective CI 95.

<i>Odontaster validus</i>				<i>Sterechinus neumayeri</i>		
Station	σ_0 (MPa)	CI 95 -	CI 95 +	σ_0 (MPa)	CI 95 -	CI 95 +
BAE	0.26a,b	0.18	0.39	4.51	3.35	6.08
WHB	0.27a	0.21	0.35	3.78	2.88	4.97
BID	0.14b	0.10	0.20	4.61	3.24	6.56
TEL	0.17a,b	0.12	0.23	4.56	3.05	6.83
Station	m	CI95% -	CI95% +	m	CI95% -	CI95% +
BAE	0.99	0.68	1.45	1.51	0.98	2.35
WHB	1.49	1.02	2.18	1.42	0.97	2.06
BID	1.17	0.80	1.72	1.10	0.75	1.59
TEL	1.22	0.84	1.79	0.99	0.67	1.46
Station	F_{max0} (N)	CI95% -	CI95% +	F_{max0} (N)	CI95% -	CI95% +
BAE	1.46b,c	1.17	1.83	0.76	0.63	0.93
WHB	2.32a	1.98	2.72	0.76	0.64	0.90
BID	1.35c	1.12	1.63	0.69	0.54	0.89
TEL	1.99a,b	1.68	2.35	0.48	0.40	0.58
Station	E_0 (GPa)	CI95% -	CI95% +	E_0 (GPa)	CI95% -	CI95% +
BAE	0.93a	0.66	1.30	0.11	0.08	0.16
WHB	0.73a,b	0.55	0.97	0.09	0.06	0.12
BID	0.41b	0.29	0.57	0.12	0.08	0.17
TEL	0.52a,b	0.39	0.70	0.13	0.09	0.21

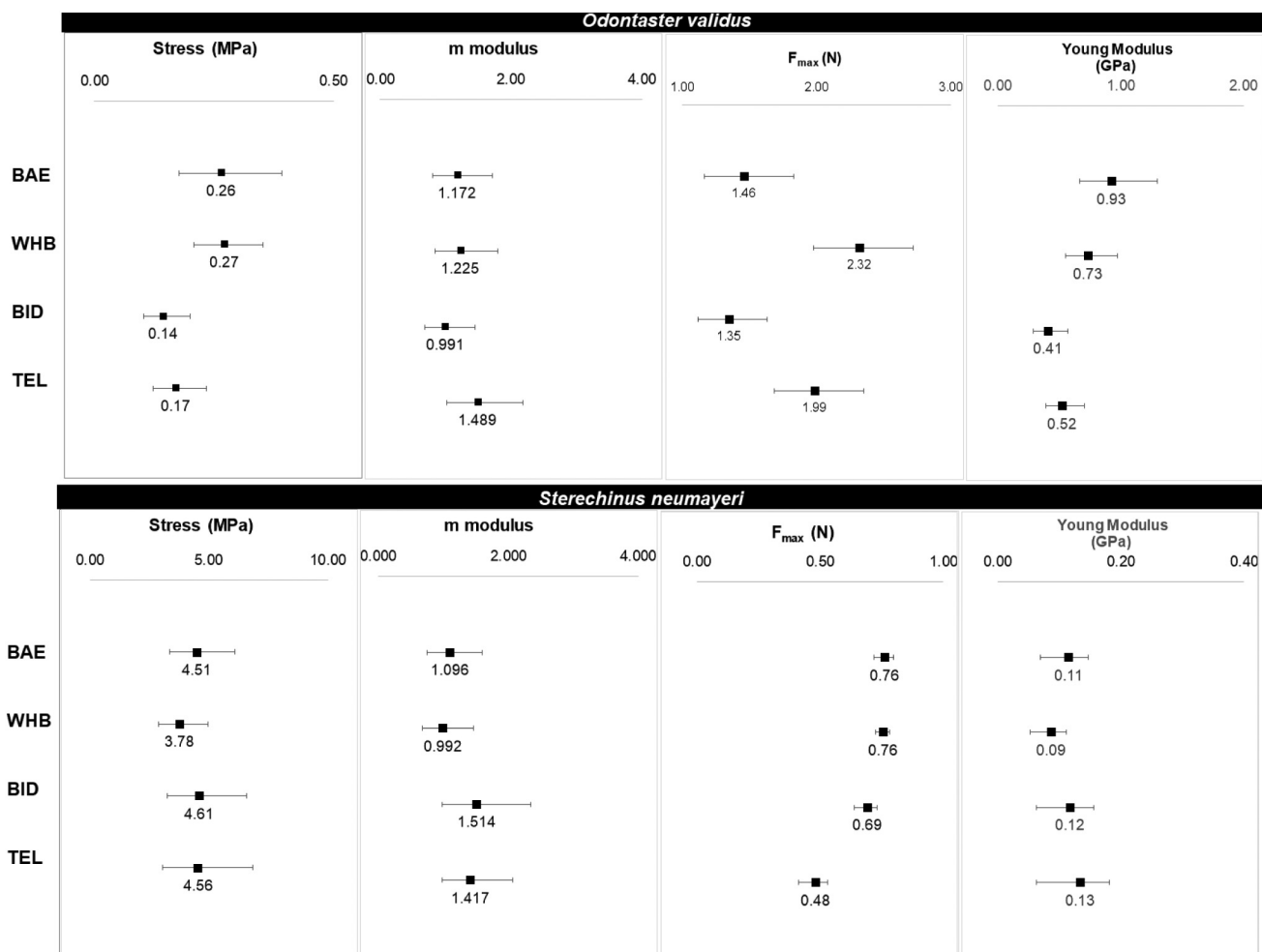


Fig. 2. Characteristic mechanical properties: stress, Weibull modulus, F_{max} and Young's modulus (E), value at which 63% of the plates break) with lower and upper 95% confidence intervals (CI) of ambulacral plates of *Odontaster validus* and interambulacral ambital plates of *Sterechninus neumayeri* at the four station of Deception Island.

characteristic stress (σ_0), the characteristic Young's modulus (E_0) and the Weibull moduli (m) were not significantly different between sea urchins from control and lower pH_{SW} stations (Table 5, Fig. 2, S08).

3.4. Metals concentration in three compartments of *O. validus* and *S. neumayeri*

In both species, metal concentrations and their rankings differed according to compartments and stations (Table 6). In *O. validus*, metal concentrations in the integument of BID sea stars departed from those of other stations, showing more positive loadings along PC2 to which Cd, Cu and Pb mainly contributed (S11 A-B, S12). Metal concentrations in the gonads and pyloric caeca of WHB sea stars departed from those of the other stations, showing more negative loadings along PC1, a dimension to which all metals contributed (S11, C–F, S12). In *S. neumayeri*, metal concentrations in the integument and digestive tract of sea urchins from all stations are clearly discriminated (S12, S13A,B,E,F). Metal concentrations in the gonads of WHB sea urchins departed from those of the other stations, showing more positive loadings along PC1, a dimension to which Zn and Cu principally contributed (S12, S13C,D).

It is noteworthy that Cd concentrations in all body parts of *O. validus* were particularly high, ranging between 8.96 and 170.85 $\mu\text{g g}_{\text{DW}}^{-1}$, while this is not the case for *S. neumayeri* in the same stations. In both species, Fe concentrations were rather high, reaching 9652 $\mu\text{g g}_{\text{DW}}^{-1}$ in the former pyloric caeca and 6261 $\mu\text{g g}_{\text{DW}}^{-1}$ in the latter digestive tract. On the contrary, Pb concentrations in all body parts of both species are rather low, being always below 1 $\mu\text{g g}_{\text{DW}}^{-1}$.

In *O. validus*, concentrations of Cu, Fe and Pb in the integument were significantly negatively correlated to the pH_{T-CF} while Cd concentrations were significantly positively correlated with pH_{CF} (Table 7, S14). Correlation of Zn concentrations with pH_{CF} was not significant. In gonads,

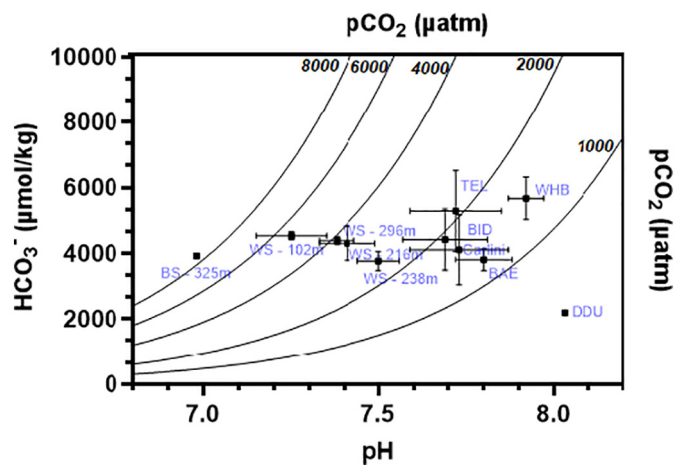


Fig. 3. pH-bicarbonate (Davenport) diagram showing differences of acid-base physiology (mean \pm SD, $n = 3$) of *Sterechninus neumayeri* at different stations and depths (15 m to 325 m) in Antarctica. BS: Bransfield Strait, WS: Weddel Sea (data from Collard et al., 2015), DDU: Dumont d'Urville (Terre-Adélie, unpublished data from Dubois Ph.), Carlini (King George Island, WAP, unpublished data from Agüera A.) and DI: Deception Island (WAP, present study). The solid curved lines represent pCO₂ isopleths.

Table 6

Metals concentrations (Cd, Cu, Fe, Pb and Zn) in different body parts of the sea star *Odontaster validus* (integument, gonads and pyloric caeca) and of the sea urchin *Sterechinus neumayeri* (integument, gonads and digestive tract) from the four stations at Deception Island (Mean \pm SD, n = 6).

		<i>Odontaster validus</i>			
		BAE	WHB	BID	TEL
Integument	[Cd] (μgg^{-1})	89.10 \pm 39.85	170.85 \pm 33.86	142.75 \pm 10.69	89.54 \pm 36.95
	[Cu] (μgg^{-1})	13.59 \pm 6.81	13.96 \pm 3.61	29.92 \pm 12.04	13.09 \pm 3.33
	[Fe] (μgg^{-1})	346.38 \pm 88.27	221.60 \pm 41.09	293.45 \pm 88.93	295.44 \pm 235.83
	[Pb] (μgg^{-1})	0.60 \pm 0.28	0.45 \pm 0.10	1.10 \pm 0.35	0.56 \pm 0.30
	[Zn] (μgg^{-1})	75.47 \pm 4.36	61.26 \pm 6.01	74.07 \pm 6.19	74.53 \pm 9.50
Gonads	[Cd] (μgg^{-1})	30.64 \pm 6.29	6.59 \pm 2.06	21.74 \pm 7.75	12.65 \pm 5.29
	[Cu] (μgg^{-1})	6.61 \pm 7.75	3.08 \pm 0.66	3.60 \pm 2.09	2.70 \pm 0.91
	[Fe] (μgg^{-1})	322.22 \pm 65.81	265.04 \pm 123.82	291.50 \pm 131.14	113.05 \pm 25.79
	[Pb] (μgg^{-1})	0.56 \pm 0.41	0.22 \pm 0.02	0.71 \pm 0.34	0.29 \pm 0.19
	[Zn] (μgg^{-1})	99.17 \pm 5.16	80.33 \pm 2.27	100.75 \pm 10.43	94.53 \pm 6.98
Pyloric caeca	[Cd] (μgg^{-1})	16.80 \pm 10.04	9.79 \pm 0.89	20.71 \pm 10.83	8.96 \pm 2.37
	[Cu] (μgg^{-1})	24.20 \pm 10.83	17.27 \pm 2.81	30.01 \pm 9.17	17.55 \pm 2.87
	[Fe] (μgg^{-1})	6916.31 \pm 2462.77	9651.78 \pm 1685.48	2229.30 \pm 508.01	662.73 \pm 157.91
	[Pb] (μgg^{-1})	0.31 \pm 0.15	0.27 \pm 0.04	0.94 \pm 0.54	0.28 \pm 0.16
	[Zn] (μgg^{-1})	386.85 \pm 97.11	94.07 \pm 25.39	371.02 \pm 91.48	414.33 \pm 50.72
		<i>Sterechinus neumayeri</i>			
		BAE	WHB	BID	TEL
Integument	[Cd] (μgg^{-1})	1.20 \pm 0.31	1.46 \pm 0.21	1.50 \pm 0.24	1.39 \pm 0.24
	[Cu] (μgg^{-1})	1.12 \pm 0.24	0.73 \pm 0.16	1.63 \pm 0.49	2.43 \pm 0.76
	[Fe] (μgg^{-1})	290.97 \pm 45.96	140.39 \pm 35.44	350.42 \pm 77.55	589.78 \pm 218.65
	[Pb] (μgg^{-1})	0.55 \pm 0.11	0.18 \pm 0.06	0.55 \pm 0.32	0.55 \pm 0.28
	[Zn] (μgg^{-1})	401.90 \pm 153.96	407.46 \pm 119.21	332.90 \pm 81.94	619.86 \pm 89.94
Gonads	[Cd] (μgg^{-1})	1.19 \pm 0.51	1.71 \pm 1.08	2.07 \pm 1.32	1.54 \pm 0.40
	[Cu] (μgg^{-1})	1.87 \pm 1.32	2.01 \pm 0.35	1.52 \pm 0.25	1.35 \pm 0.51
	[Fe] (μgg^{-1})	284.25 \pm 168.36	727.45 \pm 404.33	446.21 \pm 218.21	509.03 \pm 344.45
	[Pb] (μgg^{-1})	0.55 \pm 0.19	0.20 \pm 0.06	0.55 \pm 0.36	0.55 \pm 0.49
	[Zn] (μgg^{-1})	127.87 \pm 23.33	112.78 \pm 44.41	120.89 \pm 33.71	135.98 \pm 25.24
Digestive tract	[Cd] (μgg^{-1})	6.06 \pm 1.22	4.00 \pm 0.94	8.15 \pm 3.56	1.68 \pm 0.59
	[Cu] (μgg^{-1})	4.91 \pm 3.56	10.95 \pm 7.37	5.66 \pm 1.81	3.60 \pm 1.55
	[Fe] (μgg^{-1})	1595.45 \pm 402.50	6260.74 \pm 1322.75	3977.64 \pm 1559.87	3009.00 \pm 576.63
	[Pb] (μgg^{-1})	0.55 \pm 1.10	0.72 \pm 0.45	0.55 \pm 0.76	0.55 \pm 0.03
	[Zn] (μgg^{-1})	216.56 \pm 110.95	114.54 \pm 21.75	95.58 \pm 30.30	84.64 \pm 58.23

only Cd concentrations were significantly (negatively) correlated with pH_{CF} . No metal concentration in pyloric caeca were significantly correlated with pH_{CF} .

In *S. neumayeri*, concentrations of all metals in the integument were significantly negatively correlated to the pH_{CF} (Table 7, S15). In gonads, Pb and Zn concentrations were significantly negatively correlated with pH_{CF} while Cu concentrations were positively correlated with pH_{CF} . No metal concentration in the digestive tract was significantly correlated

Table 7

Pearson correlation coefficients and associated probabilities between $\text{pH}_{\text{T-CF}}$ and metal concentrations in the different compartments of *Odontaster validus* and *Sterechinus neumayeri*.

		Cd	Cu	Fe	Pb	Zn
		<i>Odontaster validus</i>				
Integument	pH_{CF}	0.249	-0.321	-0.390	-0.299	-0.093
	p-value	0.006	<10 ⁻³	<10 ⁻³	0.001	0.314
Gonads	pH_{CF}	-0.458	-0.209	-0.116	-0.139	-0.393
	p-value	0.024	0.326	0.591	0.518	0.057
Pyloric caeca	pH_{CF}	-0.343	-0.294	0.224	-0.157	-0.365
	p-value	0.101	0.164	0.294	0.464	0.079
		<i>Sterechinus neumayeri</i>				
Integument	pH_{CF}	-0.358	-0.642	-0.234	-0.312	-0.462
	p-value	<10 ⁻³	<10 ⁻³	0.011	0.001	<10 ⁻³
Gonads	pH_{CF}	-0.287	0.463	0.316	-0.435	-0.525
	p-value	0.175	0.023	0.132	0.034	0.008
Digestive tract	pH_{CF}	-0.261	0.341	0.331	0.098	-0.118
	p-value	0.229	0.112	0.123	0.656	0.591

with pH_{CF} . It is noteworthy that most correlation coefficients were rather low.

3.5. Relationships between pH_{CF} , metal concentrations in the integument and mechanical properties of the skeleton

Relationships between pH_{CF} , metal concentrations in the integument and mechanical properties (F_{max} , I_2 , E and stress, Table 7, S14 and S15) of the skeleton were analysed using GLM. In *O. validus*, neither stress nor Young's modulus were linked to any metal concentration or pH_{CF} ($p_{\text{Model}} = 0.61$ and 0.36 , respectively). The model was significant for F_{max} ($p_{\text{Model}} = 0.004$, $R^2 = 0.135$) although no slope of an individual factor was significant. The model was also significant for I_2 ($p_{\text{Model}} = 0.004$, $R^2 = 0.140$), with the slopes for variables "Cd concentration" (negative slope) and "Cd concentration * $\text{pH}_{\text{T-CF}}$ " (positive slope) being marginally significant ($p_{\text{coefficient}} = 0.047$). This indicates that high Cd concentrations resulted in a smaller I_2 , indicating thinner or more porous plates. In *S. neumayeri*, no mechanical variable was linked to any metal concentration or to pH_{CF} ($p_{\text{Model}} = 0.52, 0.60, 0.20$ for, respectively stress, E, and F_{max}).

4. Discussion

4.1. Sampling stations

Seawater temperature was similar in the different stations and close to open ocean values, indicating that hot vents do not influence it on a

larger scale than from the places where they are occurring. Two stations were characterized by high seawater pH_T (WHB 8.13 and BAE 8.04) and two by reduced sea water pH_T (TEL 7.82 and BID 7.77). These values are point data and a longer monitoring would be desirable. However, they correspond to those recorded in 2017 (one year before the present study) in the same stations by Angulo-Preckler et al. (2018). This suggests rather stable sea water acid-base conditions, at least at the time scale of echinoderm physiology. Because the Base Antártica Gabriel de Castilla is only operated 4 month a year and risk of ice scouring prevents the deployment of an autonomous pH recorder, obtaining year round pH data is currently impossible. Metal concentrations measured in the total fraction of the superficial sediment were lower than those measured previously in the sediment of several stations at Deception Island (Somoza et al., 2004; Deheyn et al., 2005; Guerra et al., 2011). This could be linked to the much shallower location of our samples, compared to previous studies. Indeed, Deheyn et al. (2005) showed that metal concentration in sediments are lower away from the axis of the caldera. This is probably linked to differences in sediment origin between our shallow samples and the deeper samples of previous studies (Sturz et al., 2003). Metal concentrations in sediment appeared poorly linked to water acidification. WHB, which has the highest pH_{SW} , was the most contaminated station while the three other stations showed lower metal concentrations in their sediment. Anyway, the metal concentrations measured in the sediment of WHB remained moderate compared to those measured in sediments of urbanized coasts of the Mediterranean and the North Sea (see e.g. Coteur et al., 2003) or of other Antarctic sites (Webb et al., 2020).

4.2. Acid-base physiology of *Odontaster validus* and *Sterechinus neumayeri*

The acid-base physiology of both species was here investigated for the first time. Samplings were carried out end of February, which means that all collected individuals of both species were in post-spawning stage (*O. validus* spawn from June to September and *S. neumayeri* from October to December; Pearse, 1991). This increased the homogeneity of the samplings but also reduced a possible effect of active gametogenesis on the acid-base physiology, like high protein concentration in the coelomic fluid. The sea star *O. validus* did not show differences in its acid-base variables between control and acidified stations except for a lower carbonate ion concentration in BID. Although sea stars from WHB were significantly larger than that of TEL, this did not impact their acid-base characteristics. Temperate sea stars studied so far do not compensate their coelomic fluid pH (pH_{CF}) when facing OA in laboratory experiments up to six months (Hernroth et al., 2011; Appelhans et al., 2012; Dupont and Thorndyke, 2012; Collard et al., 2013a). However, Collard et al. (2013a) showed that the pH_{CF} of small *Asterias rubens* submitted to pH_{SW} 7.7 did not differ significantly from that of specimens maintained at control $\text{pH}_{\text{T-SW}}$ 7.9. According to these authors, this was linked to the higher surface/volume ratio of small sea stars, allowing an easier elimination of respiratory CO_2 . Antarctic species have a lower metabolism when compared to tropical and temperate species (Hughes et al., 2011; Peck, 2018), resulting in a lower respiratory rate in *O. validus* than in *A. rubens* (Peck et al., 2008; Suszczewski et al., 2010; Appelhans et al., 2012, 2014; Collard et al., 2013a). Indeed, the calculated $\text{pCO}_{2\text{-CF}}$ of *O. validus* (1050–1200 μatm) was lower than that of *A. rubens* (~1500–2000 μatm ; Appelhans et al., 2012). Therefore, we suggest that the flat morphology of *O. validus*, resulting in a lower surface/volume ratio than sea stars studied so far and a consequently easier diffusion of CO_2 , together with a low oxygen consumption at temperature around 1 °C, explained the similar pH_{CF} in control and acidified sites. We hypothesize that a more severe acidification would result in a decreased pH_{CF} as observed in temperate sea star. We cannot rule out a selection or adaptation of *O. validus* populations in the caldera to hypercapnic conditions but taking into account the very long pelagic larval development of this species (ca. half a year; Shilling

and Manahan, 1994; Agüera et al., 2015) and the subsequent high gene flow between populations, this is rather unlikely.

The sea urchin *S. neumayeri* showed a lower pH_{CF} in acidified stations compared to WHB. This was not linked to a size effect as specimens from the different stations did not significantly differ for this variable. The lower pH_{CF} recorded in acidified stations is surprising as most euechinoids were shown to compensate their pH_{CF} when facing OA (Stumpp et al., 2012a; Collard et al., 2014; Moulin et al., 2015) including close to CO_2 vents (Di Giglio et al., 2020b). This was linked to the high buffering capacity of their coelomic fluid, principally due to an accumulation of bicarbonate ions (Stumpp et al., 2012b; Collard et al., 2013b, 2014). *S. neumayeri* also has this high buffering capacity due to the high concentration in bicarbonate ions in its coelomic fluid (Collard et al., 2014; present study). A pH-bicarbonate (Davenport) diagram compiling values available for the coelomic fluid (CF) of field specimens of *S. neumayeri* clearly indicates the absence of compensation for this species, despite the high bicarbonate concentration of the CF (Fig. 3). Such absence of compensation was reported in fasting sea urchins (Stumpp et al., 2012b; Collard et al., 2013b). *S. neumayeri* feeds on algae in shallow locations and benthic detritus in deeper locations (see Michel et al., 2016, and references therein). In Deception Island, there were no macroalgae in the sampled stations and the sediment did not harbour much small macrofauna consumed by this species, like bryozoans. Therefore, sea urchins were probably detritus feeders, relying on an energetically rather poor diet. We hypothesize that the absence of pH_{CF} compensation in *S. neumayeri* in Deception Island was linked to poor food availability. The same explanation could be proposed for deep *S. neumayeri* from the Weddell Sea and Bransfield strait (Fig. 3) which were proven to be detritus feeders (Michel et al., 2016). This should be experimentally tested either in aquarium conditions or by caging experiments in Deception Island sites, with some sea urchins being offered macroalgae as food and others not.

So, in summary, the recorded acid-base physiologies of both species can be interpreted in the framework of known physiologies of temperate and tropical sea stars and sea urchins, but the moderate pH reduction in the acidified sites as well as possibly confounding factors like food shortage, prevent a definitive conclusion about the physiological answers to acidification of these two Antarctic species.

4.3. Mechanical properties of the skeleton of *Odontaster validus* and *Sterechinus neumayeri*

Mechanical properties of ambital plates of *S. neumayeri* were related neither to pH nor to metal contamination. In most temperate and tropical sea urchins, ambital plates were also shown to be resistant to OA (Holtmann et al., 2013; Moulin et al., 2015; Collard et al., 2016; Di Giglio et al., 2020b). Therefore, from this point of view, the response from *S. neumayeri* was similar to other sea urchins. In *O. validus*, ambulacral plates of specimens from BID had reduced mechanical properties compared to those of WHB (s_0 , $F_{\text{max}0}$, E_0). However, neither s_0 nor E_0 appeared linked to pH_{SW} or metal concentrations. $F_{\text{max}0}$ was weakly linked ($R^2 > 0.14$) to metal contamination and pH_{SW} but no individual factor was significant and this effect is due to an impact of Cd on the plate I_2 , indicating thinner or more porous plates. In the temperate *A. rubens*, Pb and Cd were shown to be linked to reduced F_{max} and Young's modulus (E) but this was not due to a reduced I_2 (Moureaux et al., 2011). In the latter study, Pb contamination of the ambulacral plates was much higher (up to 37.6 $\mu\text{g g}_{\text{DW}}^{-1}$) but Cd contamination was much lower (up to 7.1 $\mu\text{g g}_{\text{DW}}^{-1}$). From the present study, it appears that Cd has only a minor effect on I_2 , probably through an impact on plate growth (see Moureaux et al., 2011, for a discussion). Therefore, in the investigated sites of Deception Island, pH and metals do not have a major impact on the mechanical properties of the two investigated species, despite extremely high Cd concentrations (up to 171 $\mu\text{g g}_{\text{DW}}^{-1}$ in *O. validus*).

The skeleton of both species presented lower mechanical values than what was usually measured in the skeleton of temperate and tropical species. The Young's modulus of *O. validus* ambulacral plates is ten to twenty times lower than that of the temperate *A. rubens* from a metal contaminated station (Sørfjorden, Norway; Moureaux et al., 2011) (See Supplementary Table S16 for a review of literature). The Young's modulus, F_{max} and I_2 of the ambital plates of *S. neumayeri* are almost three orders of magnitude lower than those of the temperate *Paracentrotus lividus*, measured by Collard et al. (2016). This low skeletal resistance of Antarctic echinoderms could be linked to the low durophagous predation pressure established in Antarctic benthos from a long evolutionary time (reviewed in Peck, 2018). A second factor could be the subtidal habitat of all Antarctic echinoderms, away from wave exposure, due to ice scouring which prevents establishment and maintenance of populations in the intertidal zone and shallow subtidal. These factors would have favoured a low investment in skeleton formation at an evolutionary scale. The lower saturation state of Antarctic seawater is probably not linked to this low mechanical resistance in echinoderms as the process of calcification is not depending on carbonate ions but on bicarbonate ions (see Dubois, 2014; Collard et al., 2015, for a discussion). Besides, the major limiting factor for calcifiers is the efficient elimination of protons (Bach, 2015; Suwa et al., 2014).

For both species, food availability in the different stations might be a possible explanation for the differences observed in the skeletal properties between stations (Ebert, 2013). Food availability in the caldera is generally low (Cranmer et al., 2003) but densities of both species are high and intraspecific competition for food might be severe, especially in BID station where the highest abundances of both species were recorded (24 individuals m^{-2} for *O. validus* and 182-285 individuals m^{-2} for *S. neumayeri*) (Angulo-Preckler et al., 2017a). Low food availability and high competition could result in a lower energy allocation to skeleton formation.

4.4. Metals contamination of *Odontaster validus* and *Sterechinus neumayeri*

The ratios between metal concentrations in the compartments and the sediment ranged between 0.02 and 12. Values of Fe, Pb, Zn and Cu concentrations in the different compartments of both species were similar to values previously reported in the same species by other authors (de Moreno et al., 1997; Riva et al., 2004; Grotti et al., 2008; Webb et al., 2020). Remarkably high concentrations of cadmium for the sea star *O. validus* were recorded with 2000 times more Cd in the integument of this species than in the sediment. Such high Cd concentrations in *O. validus* were also reported by previous studies (see Webb et al., 2020, and references therein). This was attributed to the transport of the upper circumpolar deep water onto the Western Antarctic Peninsula shelf, resulting in high algal backgrounds that are transferred along the food web (Webb et al., 2020). The long life span of *O. validus* (McClintock et al., 1988) further facilitates bioaccumulation of Cd, which is in part trapped in the skeleton (Temara et al., 1997; Moureaux et al., 2011). Cd concentrations measured in *S. neumayeri* were similar to those measured by Grotti et al. (2008) in Terra Nova Bay (Ross Sea). They were much lower than those measured in another primary consumer in the WAP, the grazer *Nacella concinna* (Webb et al., 2020). This probably points out to substantial differences in food sources between the considered sites, the Deception Island benthos being poor in macroalgae.

Most metal concentrations in the integument were negatively correlated to pH_{CF} (except Cd in *O. validus*) which could indicate a higher bioavailability with decreasing pH_{SW} . However, most correlation coefficients were rather low, indicating that pH was not the main factor affecting metal bioconcentration in these species. On the contrary, no metal concentration was correlated to pH in the digestive compartments of both species. This could be linked to the naturally low pH environment of these organs, making the changes in pH_{CF} unimportant.

5. Conclusion

Although the vents of Deception Island caldera offer interesting opportunities to test hypotheses dealing with OA and metal contamination in benthic organisms, the relatively moderate pH_{SW} decrease in the studied sites as well as possibly confounding factors, principally linked to food supply and quality, are important limitations. These could be overcome by translocating organisms along the pH gradient and caging them with or without added food. These translocations should be accompanied by the deployment of a continuous pH/temperature recorder to document possible variability of the sea water pH and/or temperature during the experiment. Facilities available in the Base Antarctica Gabriel de Castilla, as well as the sheltered character of the caldera, make such experiments feasible in the future.

CRedit authorship contribution statement

S. Di Giglio: Conceptualization, Methodology, Validation, Formal analysis, Data curation, Writing - original draft, Visualization, Supervision. **A. Agüera:** Conceptualization, Writing - review & editing, Project administration. **Ph. Pernet:** Formal analysis, Data curation. **S. M'Zoudi:** Data curation. **C. Angulo-Preckler:** Investigation, Writing - review & editing. **C. Avila:** Investigation, Resources, Writing - review & editing. **Ph. Dubois:** Conceptualization, Formal analysis, Resources, Writing - review & editing, Project administration, Funding acquisition, Supervision.

Declaration of competing interest

The authors declare that they have no known competing financial interests or personal relationships that could have appeared to influence the work reported in this paper.

Acknowledgements

SD. was a holder of a FRIA grant. PD. is a Research Director of the National Fund for Scientific Research (FRS-FNRS; Belgium). This project has been feasible thanks to a collaboration with the University of Barcelona through the BLUEBIO Project (CTM2016-78901/ANT) to CA, the Spanish Station: Base Antártica Gabriel de Castilla and the Spanish Polar Committee. We would like to thank Prof. I. Eeckhaut, P. Flammang, and Mr. N. Puozzo for providing access to the SEM. The access to the IRMS for DIC measurements was provided by Prof. F. Dehairs and Dr. D. Verstraeten. We thank Blanca Figuerola for the measurements of seawater parameters at several stations of Deception Island. We thank two anonymous reviewers for their constructive comments. The study was supported by FNRS grant n° J.0219.16 SOFTECHI. This is contribution no. 012 to the RECTO project (contract no. BR/154/A1/RECTO). This is an AntECO (SCAR) contribution.

Appendix A. Supplementary data

Supplementary data to this article can be found online at <https://doi.org/10.1016/j.scitotenv.2020.142669>.

References

- Agüera, A., Collard, M., Jossart, Q., Moreau, C., Danis, B., 2015. Parameter estimations of dynamic energy budget (DEB) model over the life history of a Key Antarctic species: the Antarctic Sea star *Odontaster validus* Koehler, 1906. *PLoS One* 10, e0140078. <https://doi.org/10.1371/journal.pone.0140078>.
- Andersson, A.J., MacKenzie, F.T., Lerman, A., 2005. Coastal ocean and carbonate systems in the high CO₂ world of the anthropocene. *Am. J. Sci.* 305, 875-918. <https://doi.org/10.2475/ajs.305.9.875>.
- Angulo-Preckler, C., Leiva, C., Avila, C., Taboada, S., 2017a. Macroinvertebrate communities from the shallow soft-bottoms of Deception Island (Southern Ocean): a paradise for opportunists. *Mar. Environ. Res.* 127, 62-74. <https://doi.org/10.1016/j.marenvres.2017.03.008>.

- Angulo-Preckler, C., Tuya, F., Avila, C., 2017b. Abundance and size patterns of echinoderms in coastal soft-bottoms at Deception Island (South Shetland Islands, Antarctica). *Cont. Shelf Res.* 137, 131–141. <https://doi.org/10.1016/j.csr.2016.12.010>.
- Angulo-Preckler, C., Figueroa, B., Núñez-Pons, L., Moles, J., Martín-Martín, R., Rull-Lluch, J., Gómez-Garreta, A., Avila, C., 2018. Macrobenthic patterns at the shallow marine waters in the caldera of the active volcano of Deception Island, Antarctica. *Cont. Shelf Res.* 157, 20–31. <https://doi.org/10.1016/j.csr.2018.02.005>.
- Appelhans, Y., Thomsen, J., Pansch, C., Melzner, F., Wahl, M., 2012. Sour times: seawater acidification effects on growth, feeding behaviour and acid–base status of *Asterias rubens* and *Carcinus maenas*. *Mar. Ecol. Prog. Ser.* 459, 85–98. <https://doi.org/10.3354/meps09697>.
- Appelhans, Y.S., Thomsen, J., Opitz, S., Pansch, C., Melzner, F., Wahl, M., 2014. Juvenile sea stars exposed to acidification decrease feeding and growth with no acclimation potential. *Mar. Ecol. Prog. Ser.* 509, 227–239. <https://doi.org/10.3354/meps10884>.
- Arntz, W.E., Gallardo, V.A., 1994. Antarctic benthos: present position and future prospects. *Antarct. Sci.* 243–277. https://doi.org/10.1007/978-3-642-78711-9_16.
- Bach, L.T., 2015. Reconsidering the role of carbonate ion concentration in calcification by marine organisms. *Biogeosciences* 12, 4939–4951. <https://doi.org/10.5194/bg-12-4939-2015>.
- Barnes, D.K.A., Linse, K., Enderlein, P., Smale, D., Fraser, K.P.P., Brown, M., 2008. Marine richness and gradients at Deception Island, Antarctica. *Antarct. Sci.* 20, 271–279. <https://doi.org/10.1017/S0954102008001090>.
- Bercooso, M., Prates, G., Fernández-Ros, A., Peci, L.M., de Gil, A., Rosado, B., Páez, R., Jigena, B., 2018. Caldera unrest detected with seawater temperature anomalies at Deception Island, Antarctic peninsula. *Bull. Volcanol.* 80. <https://doi.org/10.1007/s00445-018-1216-2>.
- Bray, L., Pancucci-Papadopoulou, M.A., Hall-spencer, J.M., 2014. Sea urchin response to rising pCO₂ shows ocean acidification may fundamentally alter the chemistry of marine skeletons. *Mediterr. Mar. Sci.* <https://doi.org/10.12681/mms.579>.
- Burns, W., 2008. Anthropogenic carbon dioxide emissions and ocean acidification: the potential impacts on ocean biodiversity. *Sav. Biol. Divers.* 187–202.
- Bütikofer, L., Stawarczyk, B., Roos, M., 2015. Two regression methods for estimation of a two-parameter Weibull distribution for reliability of dental materials. *Dent. Mater.* 31, e33–e50. <https://doi.org/10.1016/j.dental.2014.11.014>.
- Byrne, M., Ho, M.A., Koleits, L., Price, C., King, C.K., Virtue, P., Tilbrook, B., Lamare, M., 2013. Vulnerability of the calcifying larval stage of the Antarctic Sea urchin *Stereochinus neumayeri* to near-future ocean acidification and warming. *Glob. Chang. Biol.* 19, 2264–2275. <https://doi.org/10.1111/gcb.12190>.
- Caldeira, K., Wickett, M.E., 2003. Anthropogenic carbon and ocean pH. *Nature* 425, 365. <https://doi.org/10.1038/425365a>.
- Collard, M., Catarino, A.I., Bonnet, S., Flammang, P., Dubois, P., 2013a. Effects of CO₂-induced ocean acidification on physiological and mechanical properties of the starfish *Asterias rubens*. *J. Exp. Mar. Biol. Ecol.* 446, 355–362. <https://doi.org/10.1016/j.jembe.2013.06.003>.
- Collard, M., Laitat, K., Moulin, L., Catarino, A.I., Grosjean, P., Dubois, P., 2013b. Buffer capacity of the coelomic fluid in echinoderms. *Comp. Biochem. Physiol. - A Mol. Integr. Physiol.* 166, 19–206. <https://doi.org/10.1016/j.cbpa.2013.06.002>.
- Collard, M., Dery, A., Dehairs, F., Dubois, P., 2014. Comparative biochemistry and physiology, part A: euechinozoa and cidarozoa respond differently to ocean acidification. *Comp. Biochem. Physiol. Part A* 174, 45–55. <https://doi.org/10.1016/j.cbpa.2014.04.011>.
- Collard, M., De Ridder, C., David, B., Dehairs, F., Dubois, P., 2015. Could the acid–base status of Antarctic Sea urchins indicate a better-than-expected resilience to near-future ocean acidification? *Glob. Chang. Biol.* 21, 605–617. <https://doi.org/10.1111/gcb.12735>.
- Collard, M., Rastrick, S.P.S., Calosi, P., Demolder, Y., Dille, J., Findlay, H.S., Hall-spencer, J.M., Milazzo, M., Moulin, L., Widdicombe, S., Dehairs, F., Dubois, P., 2016. The impact of ocean acidification and warming on the skeletal mechanical properties of the sea urchin *Paracentrotus lividus* from laboratory and field observations. *ICES J.* 12. <https://doi.org/10.1093/icesjms/fsv018>.
- Constable, A.J., Melbourne-Thomas, J., Corney, S.P., Arrigo, K.R., Barbraud, C., Barnes, D.K., ... Davidson, A.T., 2014. Climate change and Southern Ocean ecosystems I: how changes in physical habitats directly affect marine biota. *Glob. Chang. Biol.* 20 (10), 3004–3025. <https://doi.org/10.1111/gcb.12623>.
- Coteur, G., Gosselin, P., Wantier, P., Chambost-Manciet, Y., Danis, B., Pernet, P., Warnau, M., Dubois, P., 2003. Echinoderms as bioindicators, bioassays, and impact assessment tools of sediment-associated metals and PCBs in the North Sea. *Arch. Environ. Contam. Toxicol.* 45, 190–202. <https://doi.org/10.1007/s00244-003-0199-x>.
- Cranmer, T.L., Ruhl, H.A., Baldwin, R.J., Kaufmann, R.S., 2003. Spatial and temporal variation in the abundance, distribution and population structure of epibenthic megafauna in Port Foster, Deception Island. *Deep. Res. Part II Top. Stud. Oceanogr.* 50, 1821–1842. [https://doi.org/10.1016/S0967-0645\(03\)00093-6](https://doi.org/10.1016/S0967-0645(03)00093-6).
- de Moreno, J.E.A., Gerpe, M.S., Moreno, V.J., Vodopivec, C., 1997. Heavy metals in Antarctic organisms. *Polar Biol.* 17, 131–140.
- Deheyn, D.D., Gendreau, P., Baldwin, R.J., Latz, M.I., 2005. Evidence for enhanced bioavailability of trace elements in the marine ecosystem of Deception Island, a volcano in Antarctica. *Mar. Environ. Res.* 60, 1–33. <https://doi.org/10.1016/j.marenvres.2004.08.001>.
- Dell'Acqua, O., Ferrando, S., Chiantore, M., Asnaghi, V., 2019. The impact of ocean acidification on the gonads of three key Antarctic benthic macroinvertebrates. *Aquat. Toxicol.* 210, 19–29. <https://doi.org/10.1016/j.aquatox.2019.02.012>.
- DelValls, T.A., Dickson, A.G., 1998. The pH of buffers based on 2-amino-2-hydroxymethyl-1,3-propanediol ('tris') in synthetic sea water. *Deep. Res. Part I Oceanogr. Res. Pap.* 45, 1541–1554. [https://doi.org/10.1016/S0967-0637\(98\)00019-3](https://doi.org/10.1016/S0967-0637(98)00019-3).
- Di Giglio, S., Lein, E., Hu, M.Y., Stumpp, M., Melzner, F., Malet, L., Pernet, P., Dubois, P., 2020a. Skeletal integrity of a marine keystone predator (*Asterias rubens*) threatened by ocean acidification. *J. Exp. Mar. Biol. Ecol.* 526, 151335. <https://doi.org/10.1016/j.jembe.2020.151335>.
- Di Giglio, S., Spatafora, D., Milazzo, M., M'Zoudi, S., Zito, F., Dubois, P., Costa, C., 2020b. Are control of extracellular acid–base balance and regulation of skeleton genes linked to resistance to ocean acidification in adult sea urchins? *Sci. Total Environ.* 720, 137443. <https://doi.org/10.1016/j.scitotenv.2020.137443>.
- Dickson, A.G., 1990. Standard potential of the reaction: $\text{AgCl(s)} + 1/2\text{H}_2(\text{g}) = \text{Ag(s)} + \text{HCl(aq)}$, and the standard acidity constant of the ion HSO_4^- in synthetic sea water from 273.15 to 318.15 K. *J. Chem. Thermodyn.* 22, 113–127. [https://doi.org/10.1016/0021-9614\(90\)90074-Z](https://doi.org/10.1016/0021-9614(90)90074-Z).
- Dickson, A.G., Millero, F.J., 1987. A comparison of the equilibrium constants for the dissociation of carbonic acid in seawater media. *Deep Sea Res. Part, Oceanogr. Res. Pap.* 34, 1733–1743. doi:[https://doi.org/10.1016/0198-0149\(87\)90021-5](https://doi.org/10.1016/0198-0149(87)90021-5).
- Doncaster, C.P., Davey, A.J.H., 2007. Analysis of Variance and Covariance: How to Choose and Construct Models for the Life Sciences. <https://doi.org/10.1080/02664760902885203>.
- Dubois, P., 2014. The skeleton of postmetamorphic echinoderms in a changing world. *Biol. Bull.* 226, 223–236.
- Dupont, S., Thorndyke, M., 2012. Relationship between CO₂-driven changes in extracellular acid–base balance and cellular immune response in two polar echinoderm species. *J. Exp. Mar. Biol. Ecol.* 424, 32–37. <https://doi.org/10.1016/j.jembe.2012.05.007>.
- Duquette, A., Vohra, Y.K., McClintock, J.B., Angus, R.A., 2018. Near-future temperature reduces mg/Ca ratios in the major skeletal components of the common subtropical sea urchin *Lytechinus variegatus*. *J. Exp. Mar. Biol. Ecol.* 509, 1–7. <https://doi.org/10.1016/j.jembe.2018.08.007>.
- Ebert, T.A., 2013. Growth and survival of postsettlement sea urchins. *Dev. Aquac. Fish. Sci.* <https://doi.org/10.1016/B978-0-12-396491-5.00007-1> Elsevier.
- Ericson, J.A., Lamare, M.D., Morley, S.A., Barker, M.F., 2010. The response of two ecologically important Antarctic invertebrates (*Stereochinus neumayeri* and *Parborlasia corrugatus*) to reduced seawater pH: effects on fertilisation and embryonic development. *Mar. Biol.* 157, 2689–2702. <https://doi.org/10.1007/s00227-010-1529-y>.
- Fabricsius, K.E., Langdon, C., Uthicke, S., Humphrey, C., Noonan, S., De'ath, G., Okazaki, R., Muehlehner, N., Glas, M.S., Lough, J.M., 2011. Losers and winners in coral reefs acclimatized to elevated carbon dioxide concentrations. *Nat. Clim. Chang.* 1, 165–169. <https://doi.org/10.1038/nclimate1122>.
- Feely, R.A., Sabine, C.L., Lee, K., Berelson, W., Kleypas, J., Fabry, V.J., Millero, F.J., Anonymous, 2004. Impact of anthropogenic CO₂ (sub 2) on the CaCO₃ (sub 3) system in the oceans. *Science* (80-) 305, 362–366.
- Flexas, M.M., Arias, M.R., Ojeda, M.A., 2017. Hydrography and dynamics of Port Foster, Deception Island, Antarctica. *Antarct. Sci.* 29, 83–93. <https://doi.org/10.1017/S0954102016000444>.
- Foo, S.A., Sparks, K.M., Uthicke, S., Karelitz, S., Barker, M., Byrne, M., Lamare, M., 2016. Contributions of genetic and environmental variance in early development of the Antarctic Sea urchin *Stereochinus neumayeri* in response to increased ocean temperature and acidification. *Mar. Biol.* 163. <https://doi.org/10.1007/s00227-016-2903-1>.
- Gillikin, D.P., Lorrain, A., Meng, L., Dehairs, F., 2010. A Large Metabolic Carbon Contribution to the δ 13C Record in Marine Aragonitic Bivalve Shells.
- Gonzalez-Bernat, M.J., Lamare, M., Barker, M., 2012. Effects of reduced seawater pH on fertilisation, embryogenesis and larval development in the Antarctic seastar *Odontaster validus*. *Polar Biol.* <https://doi.org/10.1007/s00300-012-1255-7>.
- Grotti, M., Soggia, F., Lagomarsino, C., Riva, S.D., Goessler, W., Francesconi, K.A., 2008. Natural variability and distribution of trace elements in marine organisms from Antarctic coastal environments. *Antarct. Sci.* 20, 39–51. <https://doi.org/10.1017/S0954102007000831>.
- Guerra, R., Fetter, E., Ceschim, L.M.M., Martins, C.C., 2011. Trace metals in sediment cores from Deception and Penguin Islands (South Shetland Islands, Antarctica). *Mar. Pollut. Bull.* 62, 2571–2575. <https://doi.org/10.1016/j.marpolbul.2011.08.012>.
- Gutt, J., Starmans, A., Dieckmann, G., 1998. Phytodetritus deposited on the Antarctic shelf and upper slope: its relevance for the benthic system. *J. Mar. Syst.* 17, 435–444. [https://doi.org/10.1016/S0924-7963\(98\)00054-2](https://doi.org/10.1016/S0924-7963(98)00054-2).
- Hall-Spencer, J.M., Rodolfo-Metalpa, R., Martin, S., Ransome, E., Fine, M., Turner, S.M., Rowley, S.J., Tedesco, D., Buia, M.-C., 2008. Volcanic carbon dioxide vents show ecosystem effects of ocean acidification. *Nature* 454, 96–99. <https://doi.org/10.1038/nature07051>.
- Hernroth, B., Baden, S., Thorndyke, M., Dupont, S., 2011. Immune suppression of the echinoderm *Asterias rubens* (L.) following long-term ocean acidification. *Aquat. Toxicol.* 103, 222–224. <https://doi.org/10.1016/j.aquatox.2011.03.001>.
- Holtmann, W.C., Stumpp, M., Gutowska, M.A., Syr, S., Himmerkus, N., Melzner, F., Bleich, M., 2013. Maintenance of coelomic fluid pH in sea urchins exposed to elevated CO₂: the role of body cavity epithelia and stereom dissolution. *Mar. Biol.* 160, 2631–2645. <https://doi.org/10.1007/s00227-013-2257-x>.
- Hughes, S.J.M., Ruhl, H.A., Hawkins, L.E., Hauton, C., Boorman, B., Billett, D.S., 2011. Deep-sea echinoderm oxygen consumption rates and an interclass comparison of metabolic rates in Asterozoa, Crinozoa, Echinozoa, Holothurozoa and Ophiurozoa. *J. Exp. Biol.* 214 (15), 2512–2521. <https://doi.org/10.1242/jeb.055954>.
- Ingels, J., Vanreusel, A., Brandt, A., Catarino, A.I., David, B., De Ridder, C., Dubois, P., Gooday, A.J., Martini, P., Pasotti, F., Robert, H., 2012. Possible effects of global environmental changes on Antarctic benthos: a synthesis across five major taxa. *Ecol. Evol.* 2, 453–485. <https://doi.org/10.1002/ece3.96>.
- IPCC, 2014. Intergovernmental panel on climate change. Climate change 2014 synthesis report.
- Jewett, L., Romanou, A., 2017. Ocean acidification and other ocean changes. *Clm. Sci. Spec. Rep. Fourth Natl. Clim. Assessment II*, 364–392. <https://doi.org/10.7930/JOQV3JQB>.
- Kapsenberg, L., Hofmann, G.E., 2014. Signals of resilience to ocean change: high thermal tolerance of early stage Antarctic sea urchins (*Stereochinus neumayeri*) reared under present-day and future pCO₂ and temperature. *Polar Biol.* 37. <https://doi.org/10.1007/s00300-014-1494-x>.
- Kroeker, K.J., Micheli, F., Gambi, M.C., 2012. Ocean acidification causes ecosystem shifts via altered competitive interactions. *Nat. Clim. Chang.* 3, 156–159. <https://doi.org/10.1038/nclimate1680>.

- Kusakabe, M., Nagao, K., Ohba, T., Seo, J.H., Park, S.H., Lee, J.I., Park, B.K., 2009. Noble gas and stable isotope geochemistry of thermal fluids from deception island. *Antarctica*. *Antarct. Sci.* 21, 255–267. <https://doi.org/10.1017/S0954102009001783>.
- Linares, C., Vidal, M., Canals, M., Kersting, D.K., Amblas, D., Navarro, E., Cebrián, E., Delgado-Huertas, A., Díaz, D., Garrabou, J., Hereu, B., Avallaro, L., Teixidó, N., Ballesteros, E., 2015. Persistent natural acidification drives major distribution shifts in marine benthic ecosystems. *Proc. R. Soc. B Biol. Sci.* 282, 20150587. <https://doi.org/10.1098/rspb.2015.0587>.
- Lovell, L.L., Trego, K.D., 2003. The epibenthic megafaunal and benthic infaunal invertebrates of port Foster, Deception Island (South Shetland Islands, Antarctica). *Deep. Res. Part II Top. Stud. Oceanogr.* 50, 1799–1819. [https://doi.org/10.1016/S0967-0645\(03\)00087-0](https://doi.org/10.1016/S0967-0645(03)00087-0).
- Marsh, G., 2008. Seawater pH and anthropogenic carbon dioxide. *arXiv Prepr. arXiv0810.3596* 1–15.
- Massom, R.A., Stammerjohn, S.E., 2010. Antarctic Sea ice change and variability e physical and ecological implications. *Polar Sci.* 4, 149–186. <https://doi.org/10.1016/j.polar.2010.05.001>.
- McClintock, J.B., Pearce, J.S., Bosch, I., 1988. Population structure and energetics of the shallow-water Antarctic sea star *Odontaster validus* in contrasting habitats. *Mar. Biol.* 99 (2), 235–246.
- McClintock, J.B., Amsler, M.O., Angus, R.A., Challenger, R.C., Schram, J.B.S., Amsler, C.D., Mah, C.L., Cuce, J., Baker, B.J., 2011. The mg-calcite composition of Antarctic echinoderms: important implications for predicting the impacts of ocean acidification. *J. Geol.* 119, 457–466.
- McNeil, B.L., Matear, R.J., 2008. Southern Ocean acidification: a tipping point at 450-ppm atmospheric CO₂. *Proc. Natl. Acad. Sci. U. S. A.* 105, 18860–18864. <https://doi.org/10.1073/pnas.0806318105>.
- Mehrbach, C., Culbertson, C.H., Hawley, J.E., Pytkowicz, R.M., 1973. Measurement of the apparent dissociation constants of carbonic acid in seawater at atmospheric pressure. *Limnol. Oceanogr.* 18, 897–907. <https://doi.org/10.4319/lo.1973.18.6.0897>.
- Michel, L.N., David, B., Dubois, P., Lepoint, G., De Ridder, C., 2016. Trophic plasticity of Antarctic echinoids under contrasted environmental conditions. *Polar Biol.* 39, 913–923. <https://doi.org/10.1007/s00300-015-1873-y>.
- Millero, F.J., Woosley, R., Ditrolio, B., Waters, J., 2009. Effect of ocean acidification on the speciation of metals in seawater. *Oceanography*. <https://doi.org/10.5670/oceanog.2009.98>.
- Monteiro, T., Kerr, R., Orselli, I.B.M., Lencina-Avila, J.M., 2020. Towards an intensified summer CO₂ sink behaviour in the Southern Ocean coastal regions. *Prog. Oceanogr.* 102267. <https://doi.org/10.1016/j.poccean.2020.102267>.
- Montes-Hugo, M., Doney, S.C., Ducklow, H.W., Fraser, W., Martinson, D., Stammerjohn, S.E., Schofield, O., 2009. Recent changes in phytoplankton communities associated with rapid regional climate change along the Western Antarctic peninsula. *Science* (80-.) 323, 1470–1473. <https://doi.org/10.1126/science.1164533>.
- Morley, S.A., Suckling, C.C., Clark, M.S., Cross, E.L., Peck, L.S., 2016. Long-term effects of altered pH and temperature on the feeding energetics of the Antarctic Sea urchin, *Sterechnus neumayeri*. *Biodiversity* 17, 34–45. <https://doi.org/10.1080/14888386.2016.1174956>.
- Morse, J.W., Andersson, A.J., Mackenzie, F.T., Blake, D.F., Peacor, D.R., Allard, L.F., Berman, A., Addadi, L., Weiner, S., Tsafnat, N., Fitz Gerald, J.D., Le, H.N., Stachurski, Z.H., Iglukowska, A., Najorka, J., Voronkov, A., Chelchowski, M., Kukliński, P., Ihli, J., Wong, W.C., Noel, E.H., Kim, Y.-Y., Kulak, A.N., Christenson, H.K., Duer, M.J., Meldrum, F.C., Meng, Y., Guo, Z., Yao, H., Yeung, K.W.K., Thiyagarajan, V., Märkel, K., Kubanek, F., Willgallis, A., Ma, Y., Cohen, S.R., Addadi, L., Weiner, S., Politi, Y., Arad, T., Klein, E., Weiner, S., Addadi, L., McLaughlin, K., Nezhlin, N.P., Weisberg, S.B., Dickson, A.G., Ashley, J., Booth, T., Cash, C.L., Feit, A., Gully, J.R., Howard, M., Johnson, S., Latker, A., Mengel, M.J., Robertson, G.L., Steele, A., Terriquer, L., Albeck, S., Addadi, L., Weiner, S., Fügler, A., Konrad, F., Leis, A., Dietzel, M., Mavromatis, V., Cheng, X., Varona, P.L., Olszta, M.J., Gower, L.B., Chen, P.Y., Lin, A.Y.M., Lin, Y.S., Seki, Y., Stokes, A.G., Peyras, J., Olevsky, E.A., Meyers, M.A., McKittrick, J., Naviaux, J.D., Subhas, A.V., Dong, S., Rollins, N.E., Liu, X., Byrne, R.H., Berelson, W.M., Adkins, J.F., Dong, S., Berelson, W.M., Adkins, J.F., Emlet, R.B., 2019. Ultrastructural and microanalytical results from echinoderm calcite: implications for biomineralization and diagenesis of skeletal material. *Geochim. Cosmochim. Acta* 307, 85–90. <https://doi.org/10.1016/j.jcrysgro.2007.07.006>.
- Moulin, L., Grosjean, P., Leblud, J., Batigny, A., Collard, M., Dubois, P., 2015. Long-term mesocosms study of the effects of ocean acidification on growth and physiology of the sea urchin *Echinometra mathaei*. *Mar. Environ. Res.* 103, 103–114. <https://doi.org/10.1016/j.marenvres.2014.11.009>.
- Moureaux, C., Simon, J., Mannaerts, G., Catarino, A.I., Pernet, P., Dubois, P., 2011. Effects of field contamination by metals (cd, cu, Pb, Zn) on biometry and mechanics of echinoderm ossicles. *Aquat. Toxicol.* 105, 698–707. <https://doi.org/10.1016/j.aquatox.2011.09.007>.
- Orr, J.C., Fabry, V.J., Aumont, O., Bopp, L., Doney, S.C., Feely, R.M., Gnanadesikan, A., Gruber, N., Ishida, A., Key, R.M., Lindsay, K., Maier-reimer, E., Matear, R., Monfray, P., Mouchet, A., Najjar, R.G., Plattner, G.K., Rodgers, K.B., Sabine, C.L., Sarmiento, J.L., Schlitzer, R., Slater, R.D., Totterdell, I.J., Weirig, M.F., Yamanaka, Y., Yool, A., Matear, R., Richard, 2005. Anthropogenic decline in high-Latitude Ocean carbonate by 2100. *Nature* 437, 681–686.
- Pearse, J.S., 1991. Reproduction of Antarctic benthic marine invertebrates: tempos, modes, and timing. *Integr. Comp. Biol.* 31 (1), 65–80.
- Peck, L.S., 2005. Prospects for surviving climate change in Antarctic aquatic species. *Front. Zool.* <https://doi.org/10.1186/1742-9994-2-9>.
- Peck, L.S., 2018. Antarctic marine biodiversity: adaptations, environments and responses to change. *Oceanogr. Mar. Biol.* 105–236. <https://doi.org/10.1201/9780429454455-3>.
- Peck, L., Webb, K., Miller, A., Clark, M., Hill, T., 2008. Temperature limits to activity, feeding and metabolism in the Antarctic starfish *Odontaster validus*. *Mar. Ecol. Prog. Ser.* 358, 181–189. <https://doi.org/10.3354/meps07336>.
- Pierrot, D., Lewis, E., Wallace, D.W.R., 2006. MS Excel Program Developed for CO₂ System Calculations, in: ORNL/CDIAC-105a. Carbon Dioxide Information Analysis Center. Oak Ridge National Laboratory, US Department of Energy, Oak Ridge, Tennessee.
- Rey, J., Somoza, L., Martínez-Frías, J., 1995. Tectonic, volcanic, and hydrothermal event sequence on Deception Island (Antarctica). *Geo-Marine Lett.* 15, 1–8. <https://doi.org/10.1007/BF01204491>.
- Riva, S.D., Abellosmoschi, M.L., Magi, E., Soggia, F., 2004. The utilization of the Antarctic environmental specimen bank (BCAA) in monitoring cd and hg in an Antarctic coastal area in Terra Nova Bay (Ross Sea - northern Victoria land). *Chemosphere* 56, 59–69. <https://doi.org/10.1016/j.chemosphere.2003.12.026>.
- Rogers, A.D., Frinault, B.A.V., Barnes, D.K.A., Bindoff, N.L., Downie, R., Ducklow, H.W., Friedlaender, A.S., Hart, T., Hill, S.L., Hofmann, E.E., Linse, K., McMahon, C.R., Murphy, E.J., Pakhomov, E.A., Reygoudeau, G., Staniland, I.J., Wolf-Gladrow, D.A., Wright, R., 2019. Antarctic futures: an assessment of climate-driven changes in ecosystem structure, function, and service provisioning in the Southern Ocean. *Annu. Rev. Mar. Sci.* 12, 1–34. <https://doi.org/10.1146/annurev-marine-010419-011028>.
- Sabine, C.L., Feely, R.A., Gruber, N., Key, R.M., Lee, K., Bullister, J.L., Wanninkhof, R., Wong, C.S., Wallace, D.W.R., Tilbrook, B., Millero, F.J., Peng, T.H., Kozyr, A., Ono, T., Rios, A.F., 2004. The oceanic sink for anthropogenic CO₂. *Science* (80-.) 305, 367–371. <https://doi.org/10.1126/science.1097403>.
- Schneider, C.A., Rasband, W.S., Eliceiri, K., 2012. NIH image to ImageJ: 25 years of image analysis. *Nat. Methods* 9 (7), 671–675.
- Sewell, M.A., Hofmann, G.E., 2011. Antarctic echinoids and climate change: a major impact on the brooding forms. *Glob. Chang. Biol.* 17, 734–744. <https://doi.org/10.1111/j.1365-2486.2010.02288.x>.
- Shilling, F.M., Manahan, D.T., 1994. Energy metabolism and amino acid transport during early development of Antarctic and temperate echinoderms. *Biol. Bull.* 187, 398–407. <https://doi.org/10.2307/1542296>.
- Solomon, S., Plattner, G.-K., Knutti, R., Friedlingstein, P., 2008. Irreversible climate change due to carbon dioxide emissions. *PNAS* 56, 581–592. <https://doi.org/10.1073/pnas.0812721106>.
- Somoza, L., Martínez-Frías, J., Smellie, J.L., Rey, J., Maestro, A., 2004. Evidence for hydrothermal venting and sediment volcanism discharged after recent short-lived volcanic eruptions at Deception Island, Bransfield Strait, Antarctica. *Mar. Geol.* 203, 119–140. [https://doi.org/10.1016/S0025-3227\(03\)00285-8](https://doi.org/10.1016/S0025-3227(03)00285-8).
- Steinacher, M., Joos, F., 2016. Transient Earth system responses to cumulative carbon dioxide emissions: linearities, uncertainties, and probabilities in an observation-constrained model ensemble 1071–1103. doi:<https://doi.org/10.5194/bg-13-1071-2016>.
- Stumpff, Meike, Hu, M.Y., Melzner, F., Gutowska, M.A., Dorey, N., Himmerkus, N., Holtmann, W.C., Dupont, S.T., Thorndyke, M.C., Bleich, M., 2012a. Acidified seawater impacts sea urchin larvae pH regulatory systems relevant for calcification. *Proc. Natl. Acad. Sci.* <https://doi.org/10.1073/pnas.1209174109>.
- Stumpff, M., Trübenbach, K., Brennecke, D., Hu, M.Y., Melzner, F., 2012b. Resource Allocation and Extracellular Acid – Base Status in the Sea Urchin *Strongylocentrotus droebachiensis* in Response to CO₂ Induced Seawater Acidification 111, 194–207. doi:<https://doi.org/10.1016/j.aquatox.2011.12.020>.
- Sturz, A.A., Gray, S.C., Dykes, K., King, A., Radtke, J., 2003. Seasonal changes of dissolved nutrients within and around port Foster Deception Island, Antarctica. *Deep. Res. Part II Top. Stud. Oceanogr.* 50, 1685–1705. [https://doi.org/10.1016/S0967-0645\(03\)00086-9](https://doi.org/10.1016/S0967-0645(03)00086-9).
- Suckling, C.C., Clark, M.S., Richard, J., Morley, S.A., Thorne, M.A.S., Harper, E.M., Peck, L.S., 2015. Adult acclimation to combined temperature and pH stressors significantly enhances reproductive outcomes compared to short-term exposures. *J. Anim. Ecol.* 84, 773–784. <https://doi.org/10.1111/1365-2656.12316>.
- Suszczewski, R.S.R., Janecki, T., Domanov, M.M., 2010. Starvation and chemoreception in antarctic benthic invertebrates. 37, 56–62. <https://doi.org/10.1134/S1062359010010085>.
- Sutherland, R.A., 2002. Comparison between non-residual Al, Co, Cu, Fe, Mn, Ni, Pb and Zn released by a three-step sequential extraction procedure and a dilute hydrochloric acid leach for soil and road deposited sediment. *Appl. Geochemistry* 17, 353–365. [https://doi.org/10.1016/S0883-2927\(01\)00095-6](https://doi.org/10.1016/S0883-2927(01)00095-6).
- Suwa, R., Hatta, M., Ichikawa, K., 2014. Proton-transfer reaction dynamics and energetics in calcification and decalcification. *Chem. - A Eur. J.* 1–7. <https://doi.org/10.1002/chem.201402210>.
- Temara, A., Warnau, M., Jangoux, M., Dubois, P., 1997. Factors influencing the concentrations of heavy metals in the asteroid *Asterias rubens* L. (Echinodermata). *Sci. Total Environ.* 203, 51–63. [https://doi.org/10.1016/S0048-9697\(97\)00134-4](https://doi.org/10.1016/S0048-9697(97)00134-4).
- Turner, J., Barrand, N.E., Bracegirdle, T.J., Convey, P., Hodgson, D.A., Jarvis, M., Jenkins, A., Marshall, G., Meredith, M.P., Roscoe, H., Shanklin, J., French, J., Goosse, H., Guglielmin, M., Gutt, J., Jacobs, S., Kennicutt, M.C., Masson-Delmotte, V., Mayewski, P., Navarro, F., Robinson, S., Scambos, T., Sparrow, M., Summerhayes, C., Speer, K., Klepikov, A., 2014. Antarctic climate change and the environment: an update. *Polar Res. (G. Brit.)* 50, 237–259. <https://doi.org/10.1017/S0032247413000296>.
- Tyrrill, T., 2011. Anthropogenic modification of the oceans. *Philos. Trans. A. Math. Phys. Eng. Sci.* 369, 887–908. <https://doi.org/10.1098/rsta.2010.0334>.
- Webb, A.L., Hughes, K.A., Grand, M.M., Lohan, M.C., Peck, L.S., 2020. Sources of elevated heavy metal concentrations in sediments and benthic marine invertebrates of the western Antarctic peninsula. *Sci. Total Environ.* 698, 134268. <https://doi.org/10.1016/j.scitotenv.2019.134268>.